
CHAPTER 4

PHASE BEHAVIOUR AND PROPERTIES OF MICROEMULSION IN PRESENCE OF NaCl

4.a. Preview

The systems containing surfactant, oil and water (with electrolytes) have fascinated scientists for a long time due to their extraordinary phase behavioural changes and remarkable possibilities in technological field. Among the several electrolytes exhaustively studied, the NaCl was the most exploited one and the studies involving this on different microemulsion systems are voluminous [157-160]. Such systems that split into several liquid phases are worthy of attention as prototypes to electrolyte containing systems.

In many cases microemulsions are found coexisting with excess oil, excess water or both and these formations are named by Winsor as type I, II and III respectively [32,78]. Continuous transformation of Winsor type I system to type II system is possible as a function of salinity, temperature, pressure or nature of the components [161-163]. In ionic microemulsion systems, this transformation is usually driven by increasing the salinity (Figure 4.1). At low salinity oil in water microemulsion is found in equilibrium with excess oil at the top and at high salinity water in oil microemulsion equilibrates with excess aqueous phase at the bottom. At an intermediate range of salinity, the system separates

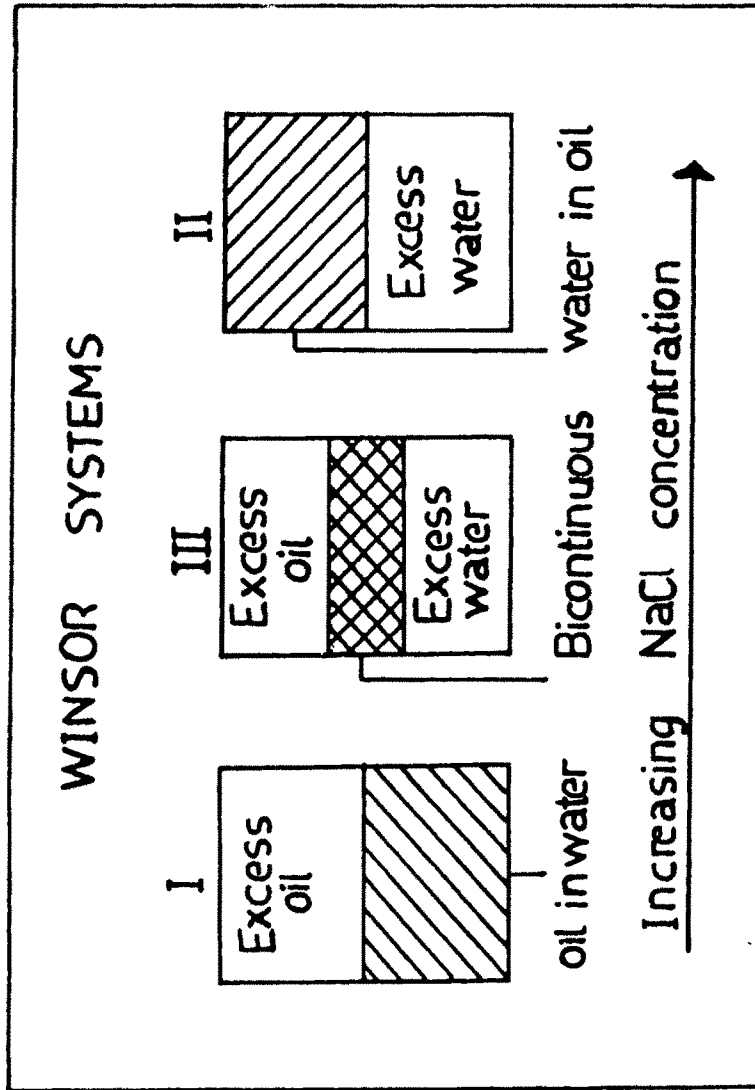


Fig.4.1 Pictorial representation of Winsor transitions I \rightarrow III \rightarrow II as the function of increasing NaCl concentration.

into three phases in which microemulsion layer is sandwiched between water layer at the bottom and oil layer at the top. In this intermediate range, where the internal microstructure is in some kind of a bicontinuous state [164], the middle microemulsion layer consists of approximately equal volumes of oil and water. In the case of microemulsions involving nonionic surfactants, the above mentioned type of transition can be visualised also by increasing the temperature of the system continuously [165,166]. Within a narrow range of temperature in the vicinity of phase inversion temperature (PIT) of the surfactant, middle phase microemulsion occurs [167]. The three phase formations are always prized for their ultralow interfacial tensions ($\sim 10^{-3}$ mN/m) prevailing between the microemulsion layer and water or oil layer. This ultralow tension is the promising factor for the employment of these formations in the oil exploration processes. Reed and Healy gave several definitions for the optimal salinity of a microemulsion system [168]. In one of them, they defined optimal salinity as the salinity at which the interfacial tension between the microemulsion phase and the excess oleic phase ($\gamma_{o/m}$) becomes equal to the interfacial tension between microemulsion phase and the excess aqueous phase ($\gamma_{m/w}$). Alternately there is the salinity at which the volume uptakes of oil and water into the middle microemulsion layer are equal. Optimising a surfactant system for better performance often involves a

large number of samples and the interfacial tension measurements for all these systems are quite tedious and time consuming. In this context, the discovery that the optimal salinity is almost the same as the salinity of equal volume uptake is important [169]. A salinity scan is perhaps the most frequently used method to find the optimal salinity of a candidate surfactant formulation.

The main purpose of this chapter is to report on the investigation of the effect of NaCl on our pseudoternary system, and to examine the Winsor transitions and optimal salinity in this system. There are many research papers dealing with the various factors influencing optimal salinity such as nature of oil, nature of cosurfactant, nature of surfactant, temperature etc. [59,170-172]. The changing parameters involved in the present study are temperature (upto as high as 80°C) and water-oil volume ratio, which are of relevance in the oil field processes. Apart from this, the effect of NaCl on the phase diagram and various properties are also studied and discussed.

4.b. Experimental

Different concentrations of aqueous NaCl solutions were taken as the aqueous phase. These solutions were prepared by diluting a 3 mol dm^{-3} NaCl solution with required amount of doubly distilled water. NaCl was dried

in an oven for two hours at 150°C and was cooled in a desiccator prior to its weighing.

4.c. Results and Discussion

(i) Phase behaviour

Figures 4.2, 4.3 and 4.4 are the illustrative pseudoternary phase diagrams of the system at 40°C obtained for 0.5, 1 and 3 mol dm⁻³ NaCl solutions as the aqueous phase respectively. The phase diagram with 0.5 mol dm⁻³ NaCl solution (fig 4.2) is similar to the diagram we obtained in the case of pure water (Chapter 3). The region marked 'X' designates the one phase isotropic region which originates from the oil corner and stretches across to the zero oil line. Comparison of this region with the corresponding region in the phase diagram of the system with water (without NaCl) shows that the region increased by about 20% of the latter. This increase may be the result of a stabilization of the microemulsion by the smaller quantity of added NaCl, as reported by Keiser et al. [52] in a detergentless microemulsion system composed of hexane, water and 2-propanol. The compositions from the region marked S/L above the solubilization region 'X' forms a solid-liquid biphasic system showing the saturated solubility of the surfactant (SDS). The region 'Y' is turbid but on standing breaks into two phases. The lower phase is water external microemulsion and the upper one is

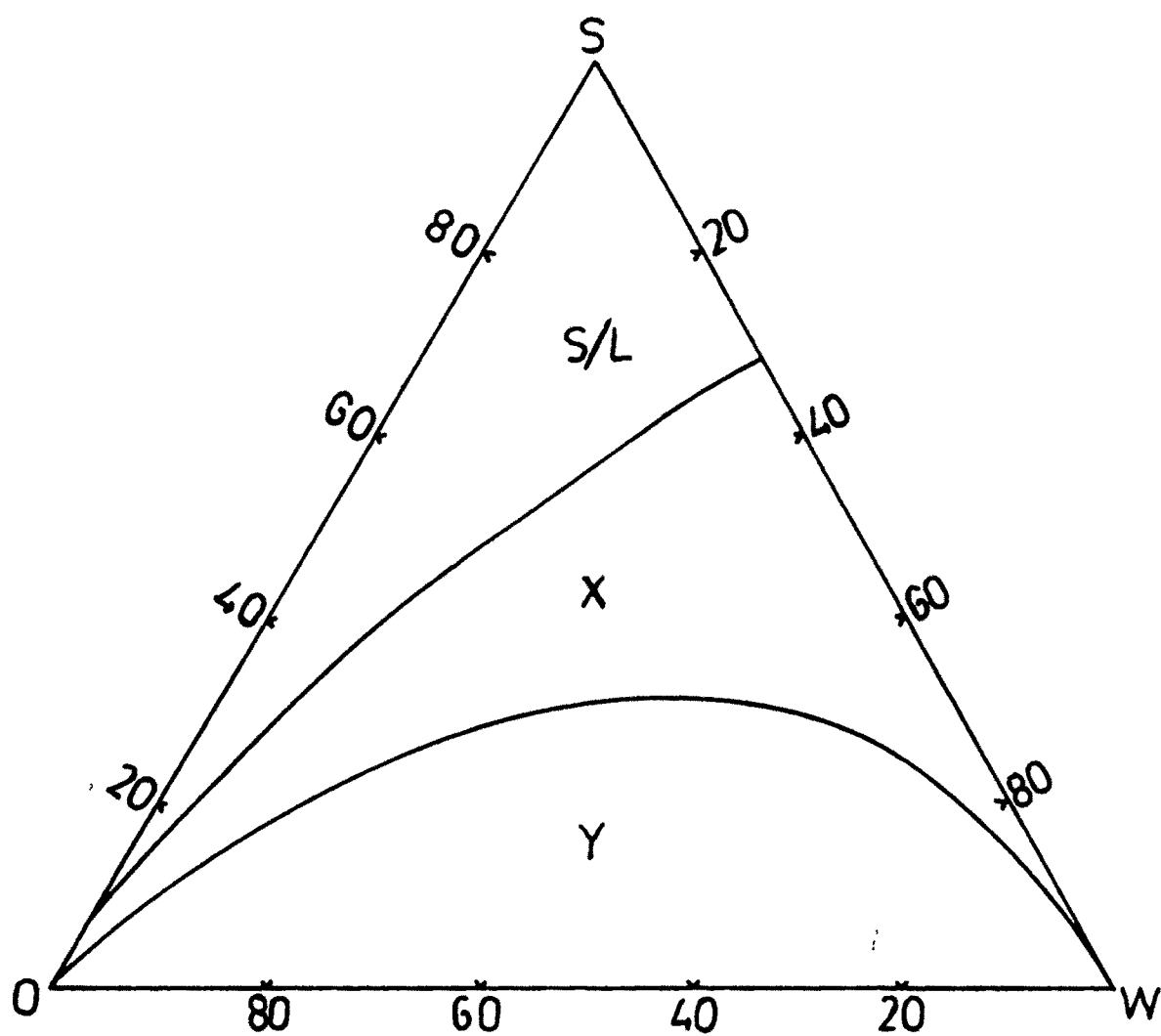


Fig. 4.2 The pseudoternary phase diagram of the system cyclohexane-SDS+propanol - 0.5 mol dm⁻³ aqueous NaCl, at 40°C. S/L solid-liquid; X single phase microemulsion, Y Winsor I.

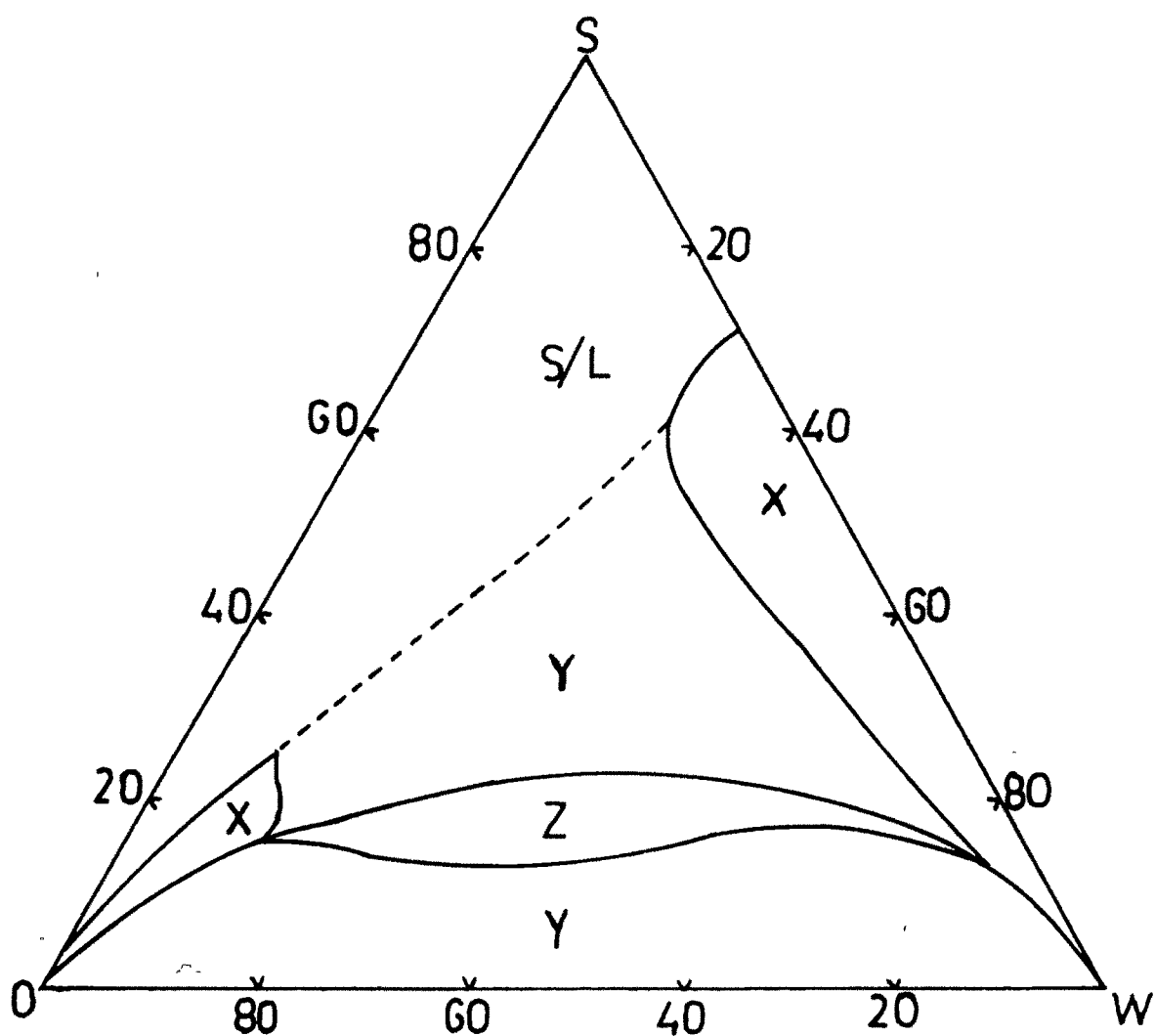


Fig.4.3 The pseudoternary phase diagram of the system cyclohexane-SDS+propanol-1 mol dm³ aqueous NaCl, at 40°C. S/L solid-liquid; X single phase microemulsion. Y Winsor I; Z Winsor III.

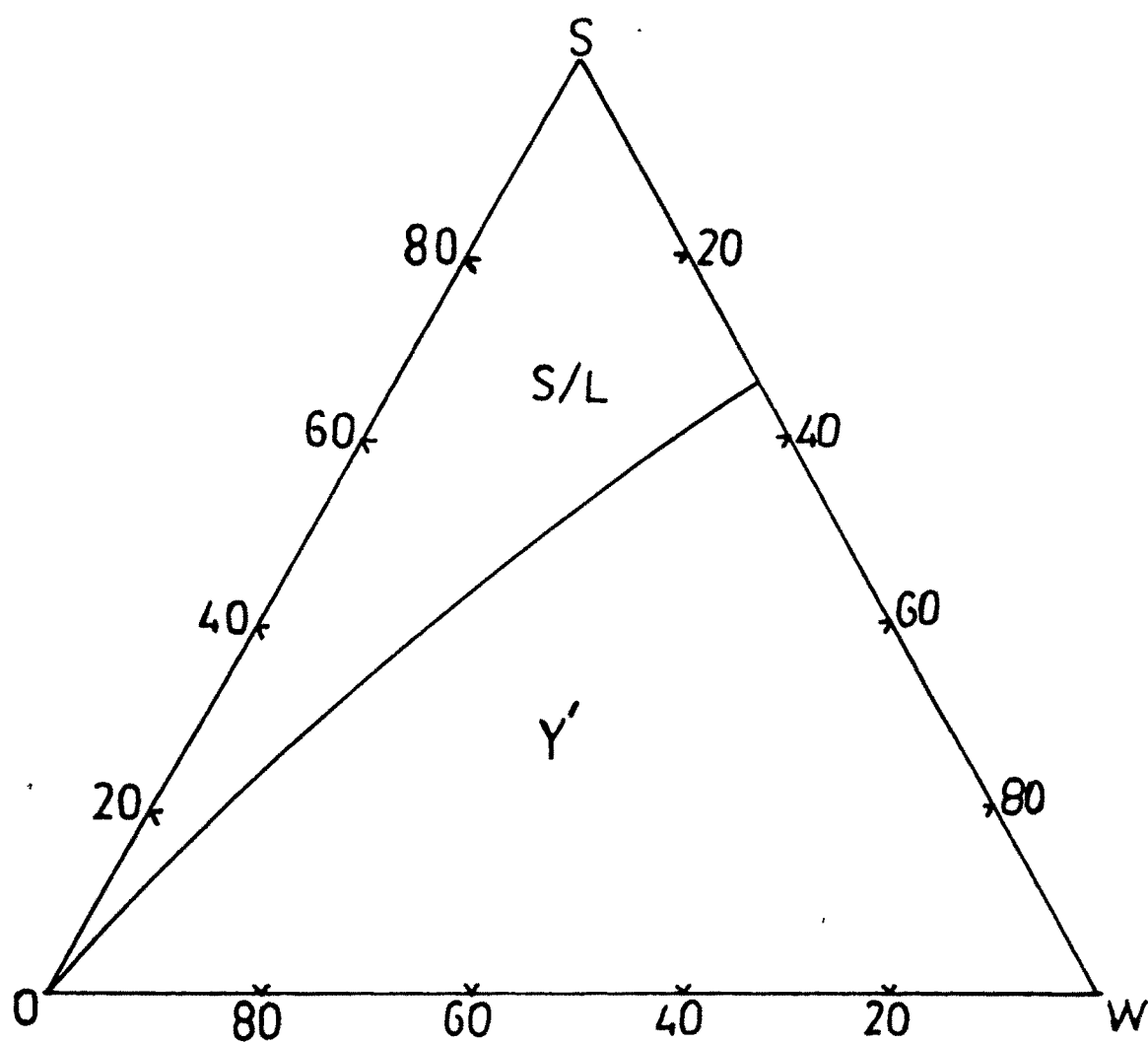


Fig.4.4 The pseudoternary phase diagram of the system cyclohexane-SDS+propanol-3 mol dm³ aqueous NaCl, at 40°C. S/L Solid-liquid; Y' Winsor II.

excess oil phase (Winsor I formation). An increase in the salinity to 1 mol dm^{-3} induces drastic changes in the phase diagram (Fig.4.3). Two disjoint one phase microemulsion zones are formed, one adjacent to the zero oil line and the other near the oil corner. Further more a three phase region (Winsor III) marked 'Z' appeared at the centre approximately around 17.5 percentage surfactant line and extend towards both the sides to meet the monophasic regions at two distinct points. At these two points it is worthy enough to note that all the three regions, i.e. monophasic, biphasic and triphasic liquid regions, coincide. All the one phase and the three phase regions disappeared from the phase diagram when the salinity of the aqueous phase was further increased to 3 mol dm^{-3} (Fig.4.4). At this concentration, phase diagram divides into two regions, a solid-liquid (S/L) region above the line drawn and a liquid-liquid region 'Y' below this line. The composition assigned to the region Y eventually breaks into two liquid layers in which the oil external microemulsion at the top is in equilibrium with excess aqueous phase at the bottom (Winsor II). The phase diagrams of all these systems (0.5 , 1 and 3 mol dm^{-3}) constructed at higher temperatures (60 and 80°C) show that these are similar to those obtained at 40°C in its general pattern. A phase prism representation of these diagrams at 80°C is given in Fig. 4.5 as a general representation.

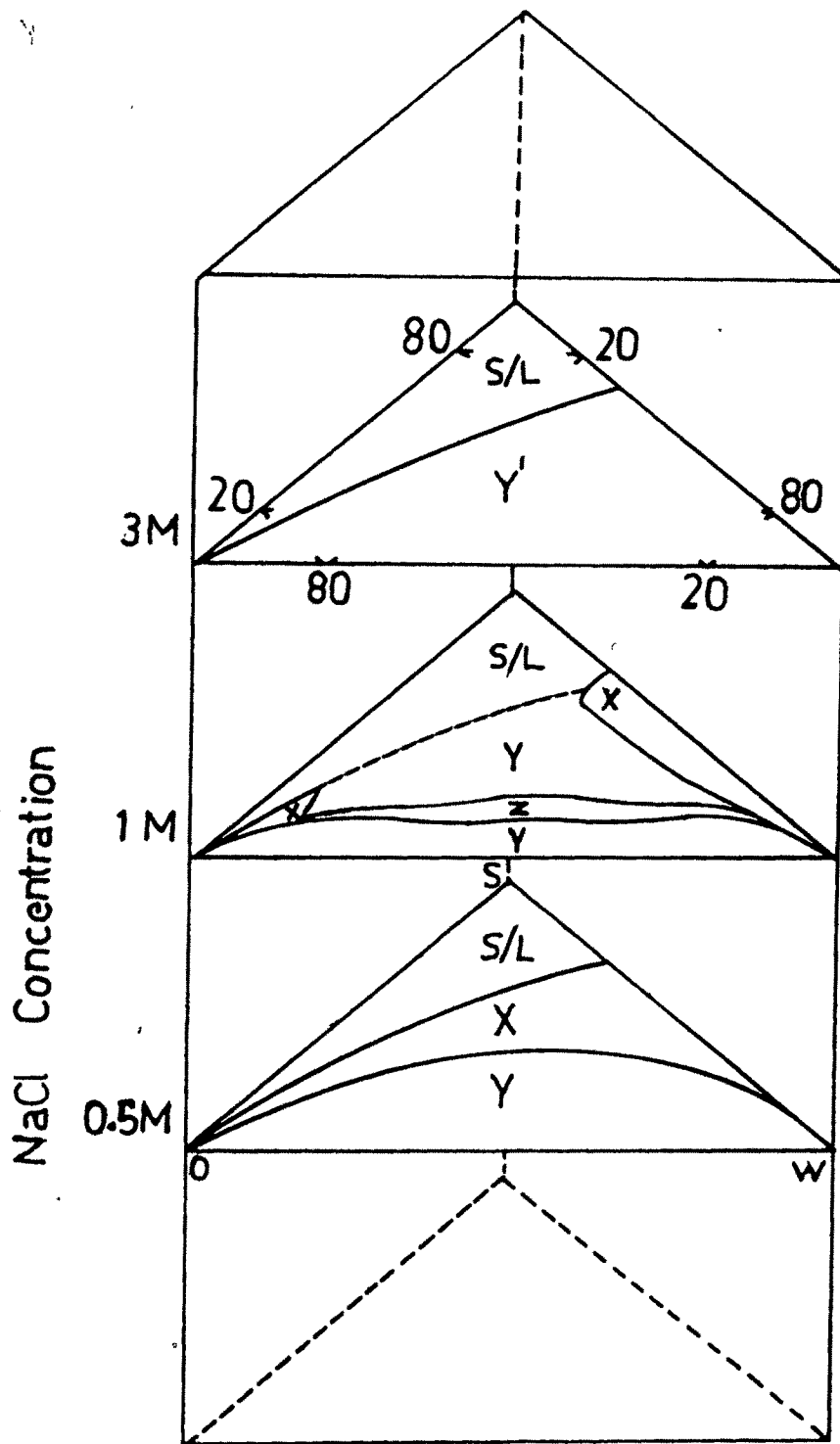


Fig.4.5 The prismatic representation of the phase diagrams obtained when water was replaced by 0.5, 1 and 3 mol dm^{-3} aqueous NaCl solutions at 80°C . S/L solid-liquid; X Single phase microemulsion; Y Winsor I; Y' Winsor II; Z Winsor III.

The formation of a water external or an oil external microemulsion is generally decided by the hydrophilic-lipophilic nature of the interfacial film created by the surfactant and cosurfactant molecules. When this interfacial layer is increasingly hydrophilic in nature a water continuous microemulsion is occurred and if this layer is increasingly hydrophobic in nature, an oil continuous microemulsion is favoured. A three phase formation is usually resulted when a surfactant system attains a favourable balance between its hydrophilicity and hydrophobicity [50]. The ionic surfactants are generally hydrophilic in nature and hence favour an oil in water type structure. But increasing concentration of electrolyte e.g. NaCl can regulate the curvature as well as the hydrophilic-lipophilic balance of the surfactant film and thus the structure in the following way. Electrical interactions between the ionic surfactant head groups can be moderated by the presence of counter ions and the electrolyte ions [173]. As the electrolytic concentration increases, the repulsive interaction between the charged head groups are further screened, the curvature of the surfactant film decreases and ultimately the droplets swell. Thus the continued salt addition eventually leads to microemulsion phase containing equal amounts of oil and water [173]. Moreover at fairly high concentration salt has another effect. Because of the

extensive solvation of relatively smaller ions of the salt, both the unfavourable interaction between water and hydrocarbon chains of the surfactant molecules and the favourable interaction between the polar head groups and water are diminished [174]. Thus the surfactant system achieves a favourable balance between its hydrophilicity and hydrophobicity to solubilize equal amounts of oil and water as middle phase microemulsion. At large ionic strength, the interaction of the surfactant head groups with water gets reduced to a level when they are outweighed by the larger entropy available in the oil phase. This will ultimately lead to the inversion of microemulsion to an oil continuous upper phase (Winsor II).

A simpler explanatory way towards the formation of Winsor I, II or III systems was provided by Aveyard et al. [161] in terms of molecular geometry of the surfactant. In this approach the cross sectional head group and tail group areas A_h and A_t are considered whose relative magnitudes determine the preferred curvature and hence microemulsion type. The first geometrical discussion of this type was made by Israelachvili, Mitchell and Ninham [175] introducing a term called packing factor of surfactant molecules which is approximately equivalent to the ratio A_t/A_h . The cross sectional areas A_h and A_t are

not the "bare" size values of an isolated surfactant molecule, but the effective areas in situ in the surfactant monolayer. There are many effects which differentiate the effective geometry from that of the isolated molecular geometry.

1. The electrostatic repulsion between neighbouring ionic head groups.
2. Solvation of the surfactant tail groups by the penetrated oil molecules.
3. Hydration of the surfactant head groups.
4. Molecular conformation effects.

In a microemulsion system, when $A_h > A_t$, the monolayer curves towards the oil phase entrapping the oil inside the surfactant sheath to form oil in water microemulsion and when $A_h < A_t$ the monolayer curves towards the aqueous phase resulting in water in oil microstructure. At an intermediary level when $A_h \sim A_t$, the average net curvature of the monolayer is close to zero and a bicontinuous type of structure will be generated.

In the present system with ionic surfactant SDS, due to the electrostatic repulsion between the two neighbouring surfactant head groups in the monolayer, they orient themselves away from each other (See Fig.4.6).

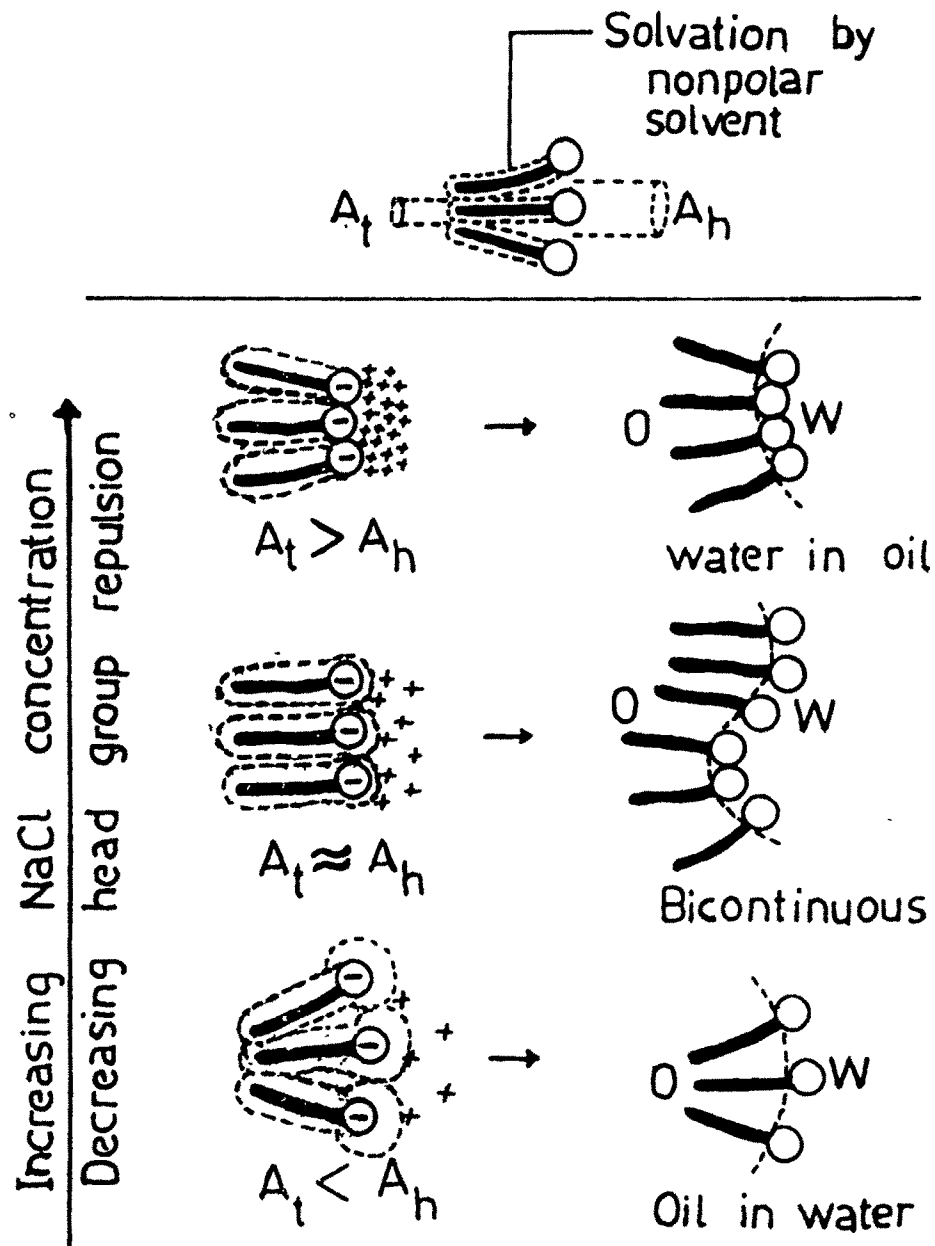


Fig.4.6 Diagrammatic representation of the variation of A_t and A_h with increasing NaCl concentration or decreasing head group repulsion.

This will produce an increase in the effective area of the head group above its "bare" size (and thereby is in a position to make $A_h > A_t$) and the microemulsion is obviously of oil in water type. The addition of an electrolyte e.g. NaCl leads to the shielding of the head group charges and hence decreases the electrostatic repulsion between the two neighbouring head groups. Thus A_h will decrease and the two head groups will be more close to each other. The simultaneous effect in the hydrocarbon tail region of the monolayer is an increased penetration by the oil molecules and thereby an increase in the effective cross sectional area of the tail A_t . When the A_h becomes approximately equal to A_t , a bicontinuous structure appears. An increased presence of electrolyte in the system will further bring down the A_h value until a stage where $A_h < A_t$ and the surfactant will prefer to encapsule the water phase and form water in oil structure.

This type of inversion from a lower phase through a middle phase to an upper phase microemulsion is seen clearly in Fig.4.7. Here the volume fraction of various layers formed, for a composition S+CS : 17.5%, 0 : 42.5% and W : 40%, is plotted against varying NaCl concentration at different temperatures. The system is biphasic approximately upto 0.95 mol dm^{-3} NaCl at 40°C and 50°C and upto 0.85 mol dm^{-3} NaCl at all the other temperatures

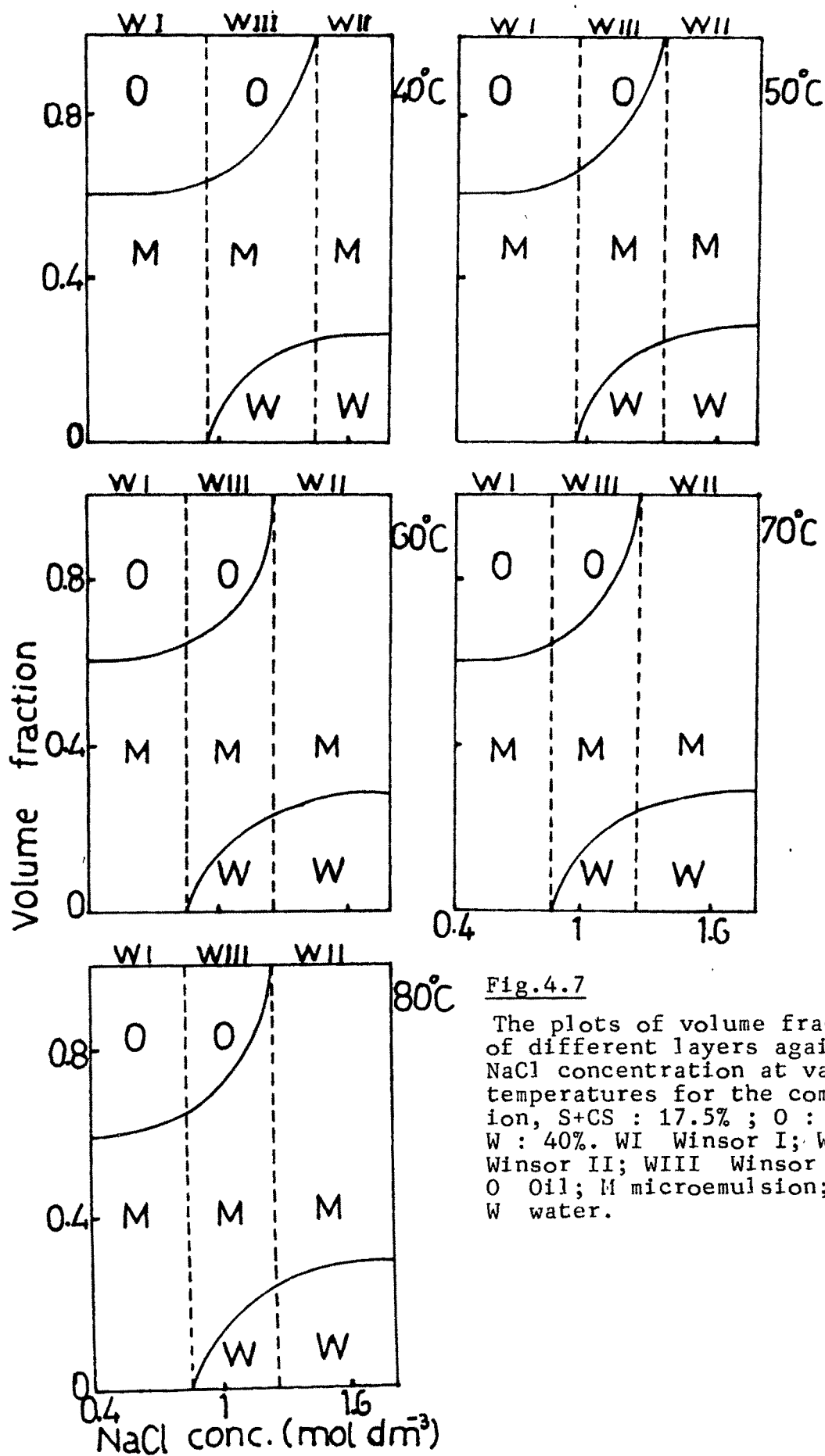


Fig.4.7

The plots of volume fraction of different layers against NaCl concentration at various temperatures for the composition, S+CS : 17.5% ; O : 42.5% ; W : 40%. WI Winsor I; WII Winsor II; WIII Winsor III; O Oil; M microemulsion; W water.

(60, 70 and 80°C) with microemulsion at the bottom and excess oil at the top. Above these concentrations, there appears three phases, the lower one is aqueous phase, the upper one is oil phase and the middle one, a bicontinuous microemulsion. On further increase in NaCl concentration, the middle microemulsion phase increases at the expense of the upper oil phase until the system reverts back to a biphasic one with microemulsion at the top and water at the bottom. These transitions occur at 1.45, 1.35, 1.25, 1.25 and 1.25 mol dm⁻³ NaCl at 40, 50, 60, 70 and 80°C respectively. It was an interesting feature to note that increase in temperature lowers the NaCl concentration at which the three phase system is formed and also narrows the concentration range at which these systems are present. In Fig.4.8 the variation in phase volume fraction of different layers, of the above particular composition, are shown as a function of increasing temperature at three constant representative salinities (0.9, 1.1 and 1.3 mol dm⁻³). In Fig.4.8a the system moves from a Winsor I to Winsor III while in Fig. 4.8c the transition occurs from Winsor III to Winsor II system. Thus it can be generalised that with increasing temperature the system moves in a direction Winsor I → Winsor III → Winsor II. (i.e. lower to middle and then to upper phase microemulsion). In other words it can be stated that the temperature increase favours the lower → middle → upper phase transition. This is quite surprising as well as contradictory to what was

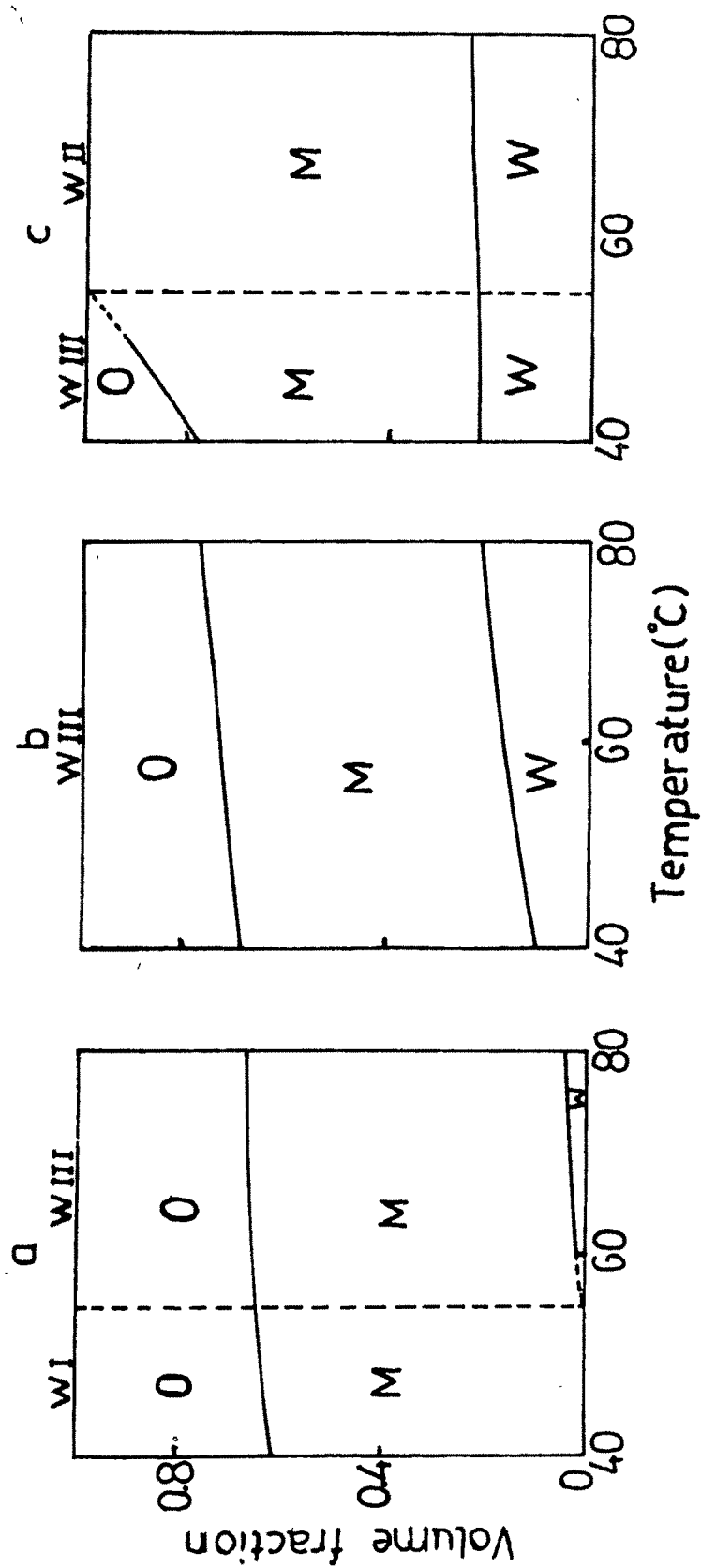


Fig. 4.8 Plots of volume fraction of different layers against temperature at three constant salinities (a) 0.9 mol dm^{-3} ; (b) 1.1 mol dm^{-3} ; and (c) 1.3 mol dm^{-3} ; symbols as in Fig 4.7.

reported and conjectured by Reed and Healy [168] where the increasing temperature induces an upper \rightarrow middle \rightarrow lower phase transition. It is well known that an increase in temperature decreases the hydrophilic property of nonionic surfactants while it increases the same of ionic surfactants [88,176]. But we attribute the observed opposite direction in transition to the increased hydrophobicity of the surfactant film and believe that it is due to the peculiar nature of the cosurfactant, propanol. Propanol is a molecule of small hydrocarbon chain. This imparts relatively high hydrophilicity to this molecule in comparison to butanol or higher alkanols. We guess this hydrophilicity is the reason for its somewhat peculiar nature. It was observed earlier that alkanols can be divided into two groups [55]. One below butanol and the other over it depending on their behaviour as co-surfactant. Most of the earlier studies were done with pentanol, hexanol etc. If V_o and V_w denote the volume uptake of oil and water phases respectively by the middle microemulsion phase and V_m the volume of microemulsion layer for a Winsor III formation, then the volume uptake ratio V_o/W_m for oil and V_w/V_m for water are called solubilization parameters of these phases [177]. The solubilization parameters of oil (V_o/V_m) and water (V_w/V_m) can be plotted together against NaCl concentration as shown in the Fig.4.9 (a & b). The concentration of NaCl

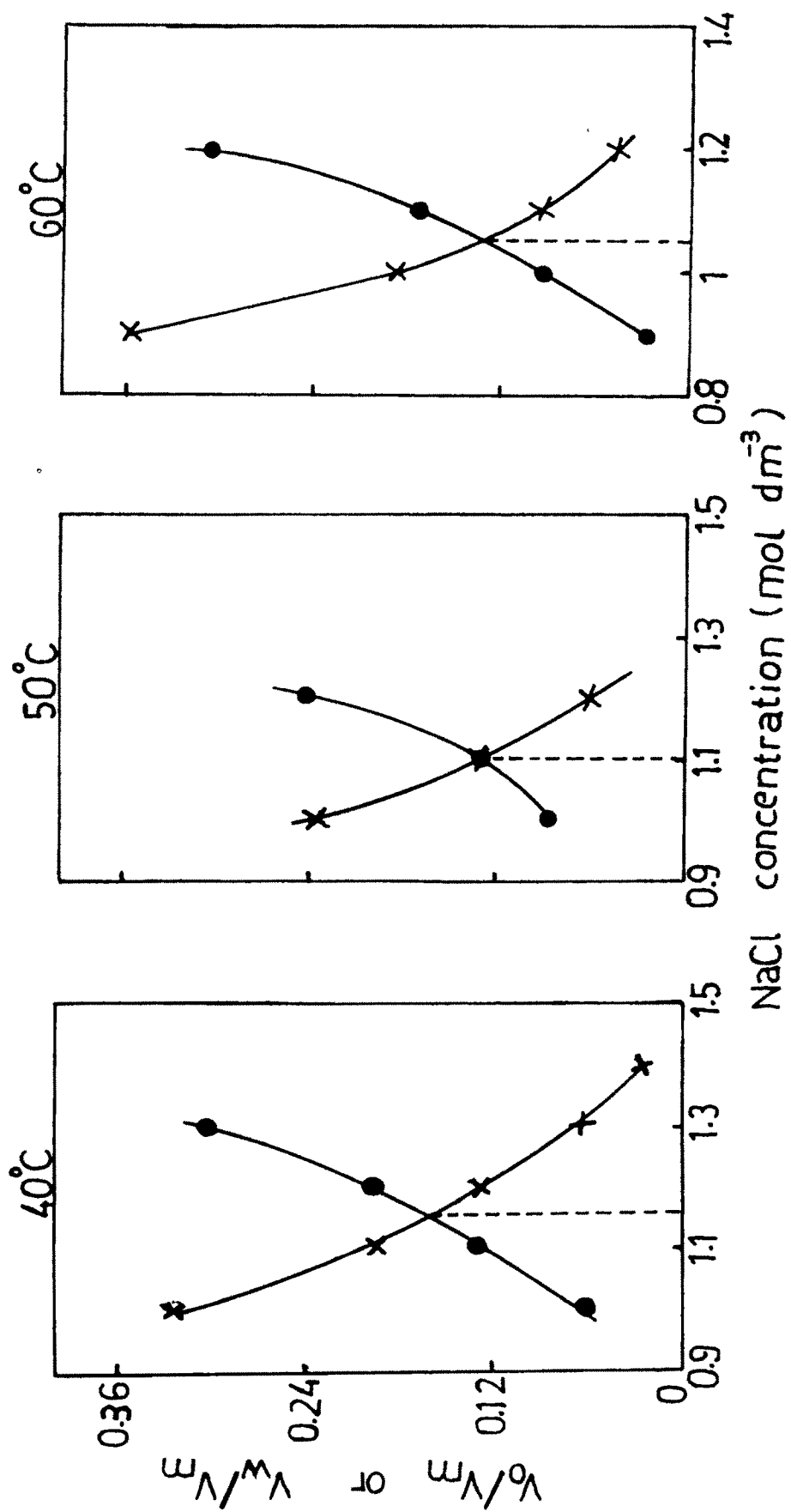


Fig.4.9a The plots of V_o/V_m \bullet and V_w/V_m \times against NaCl concentration for the composition at different temperatures.

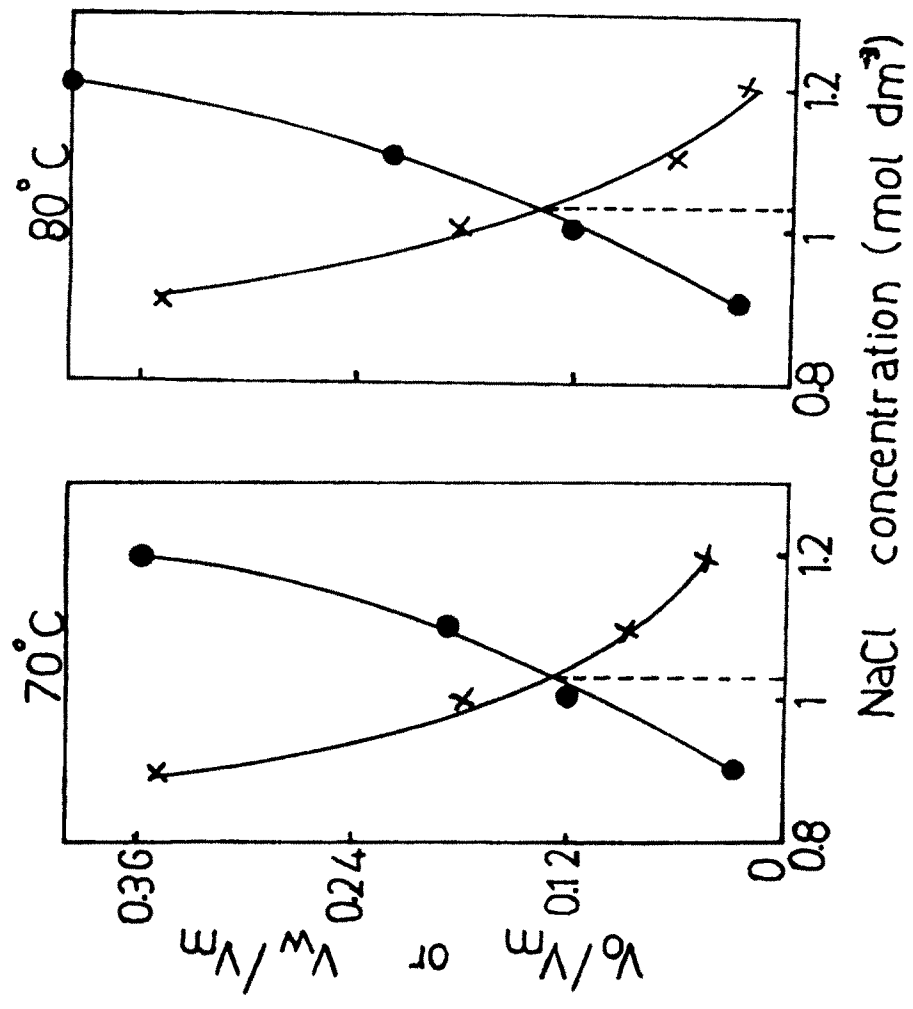


Fig.4.9b The plots of V_o/V_m ● and V_w/V_m x against NaCl concentration for the composition at 70°C and 80°C.

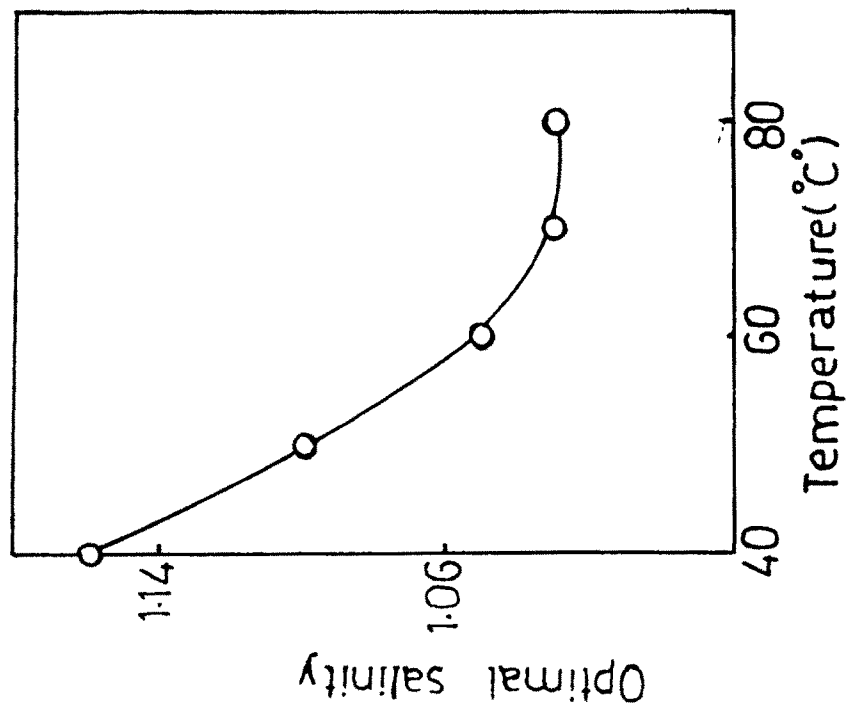


Fig.4.10 The plot of optimal salinity (mol dm⁻³) against temperature.

at which these two plots intersect corresponds to what is termed optimum salinity. The optimum salinity for the particular composition (S+CS : 17.5%, O : 42.5%, W : 40%) was determined at various increasing temperatures (Fig.4.9 a & b). Their plot against temperature (Fig.4.10) show a decline in optimum salinity with increasing temperature. Therefore the optimum salinity of microemulsion is a function of temperature. The variation is nonlinear in nature and above 70°C no further effect was observed. Since the increasing NaCl concentration and the increasing temperature are having same effect in inducing the Winsor transition (i.e. lower → middle → upper phase transition) the decrease in optimal salinity is probably the sum of these two effects in the present system.

Fig.4.11 exhibits the variation occurred in the microemulsion layer, in terms of volume fraction, when the NaCl concentration was increased continuously to produce the different Winsor formations for the composition (S+CS : 17.5%, O : 42.5%, W : 40%). At all temperatures the plots exhibit uniformity with two maxima, one at low concentration and the other at high concentration, and a very prominent minimum in between them which corresponds to the optimal salinity. Initially when the system is Winsor type I, increasing salinity dissolves more and more oil into the lower water continuous microemulsion layer. At the concentration where type III system starts forming,

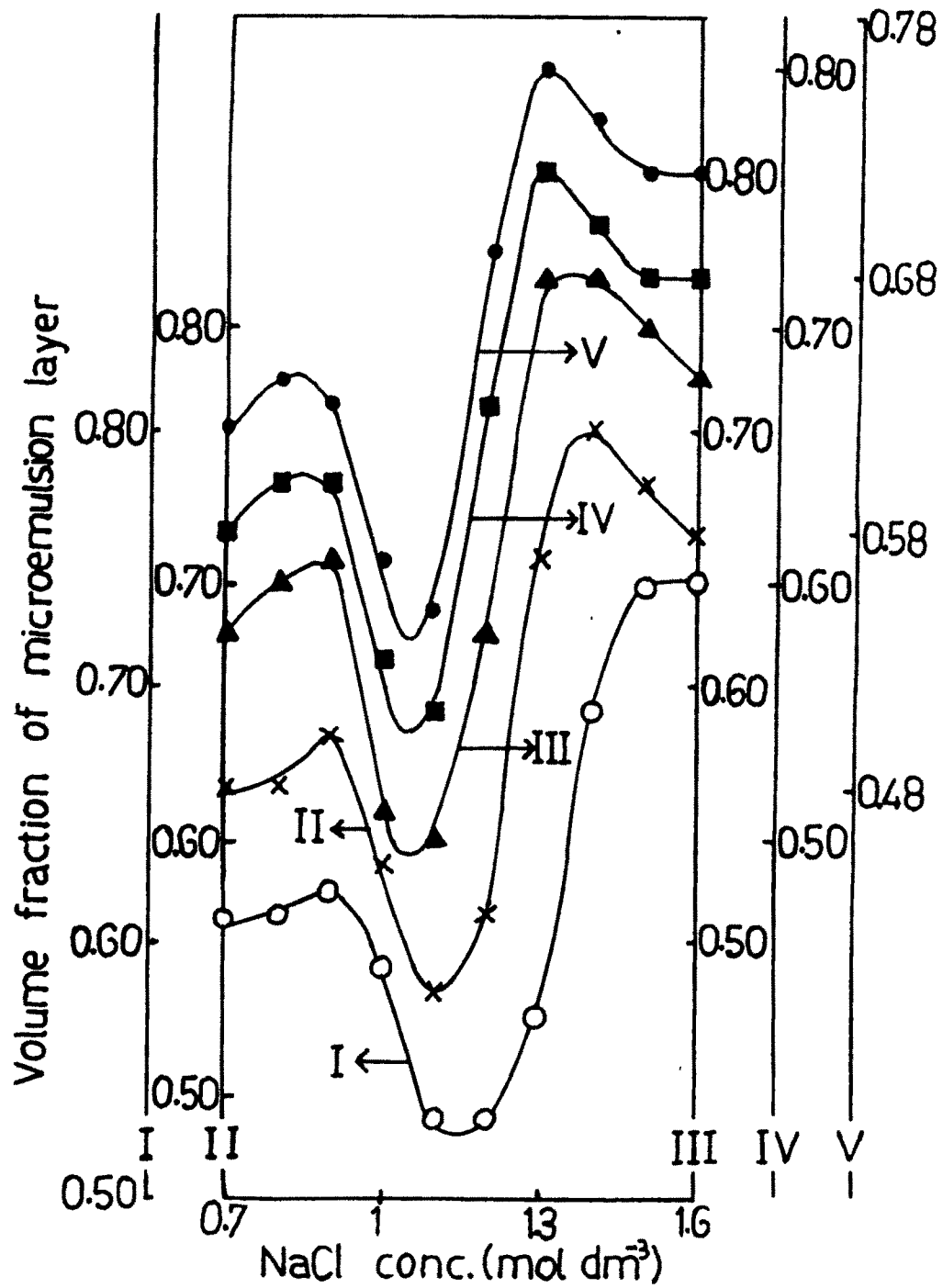


Fig.4.11 The variation of microemulsion layer volume fraction against salinity during the transition from Winsor I to Winsor II type at various temperatures. 40°C ○; 50°C ×; 60°C ▲; 70°C ■; 80°C ●.

the expulsion of water from the microemulsion layer as the excess aqueous layer commences. This water expulsion effect overcompensates the effect of oil dissolution into the microemulsion and the net effect is a sudden decrease in the volume fraction until the optimal salinity is reached. Above the optimal salinity, when the surfactant is sufficiently hydrophobic or its molecular geometry changes, the dissolution of excess oil into the microemulsion layer predominates and results in a rapid growth of the microemulsion layer. This makes the layer increasingly oil rich until the oil layer dissolves completely in the microemulsion layer. Hereafter the expulsion of more water into the lower aqueous layer causes further gradual decrease in the volume fraction of upper microemulsion layer. Hence from this study it may be stated that the overall variation in the microemulsion volume is an interplay between the oil intake and water expulsion of the microemulsion layer when the surfactant becomes increasingly hydrophobic or their molecular geometry in the monolayer changes by the addition of electrolyte.

The above mentioned type of salinity scanning and optimal salinity study was performed for various other compositions with constant surfactant weight percentage 17.5 and various water to oil ratio. Fig.4.12 correlates

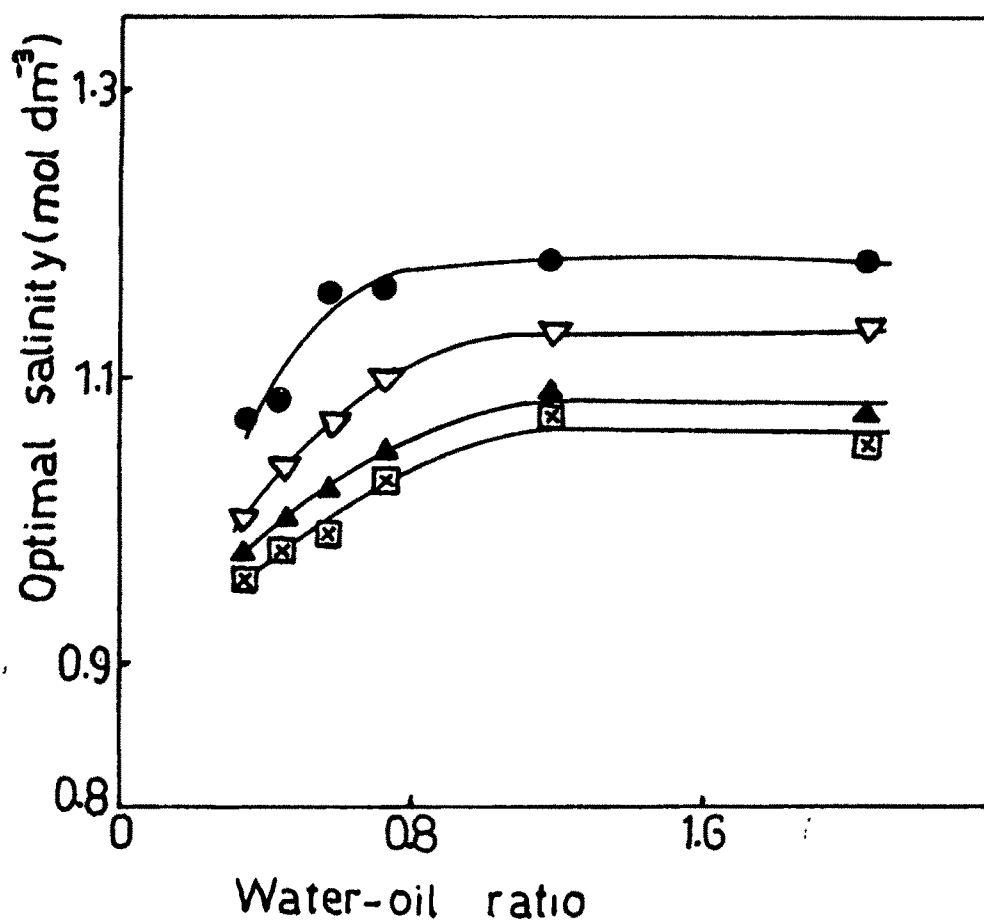


Fig.4.12 : The plots of optimal salinity against water-oil ratio at various temperatures : 40°C ●; 50°C ▼; 60°C ▲; 70°C □; 80°C ×. (70 & 80°C plots coincide).

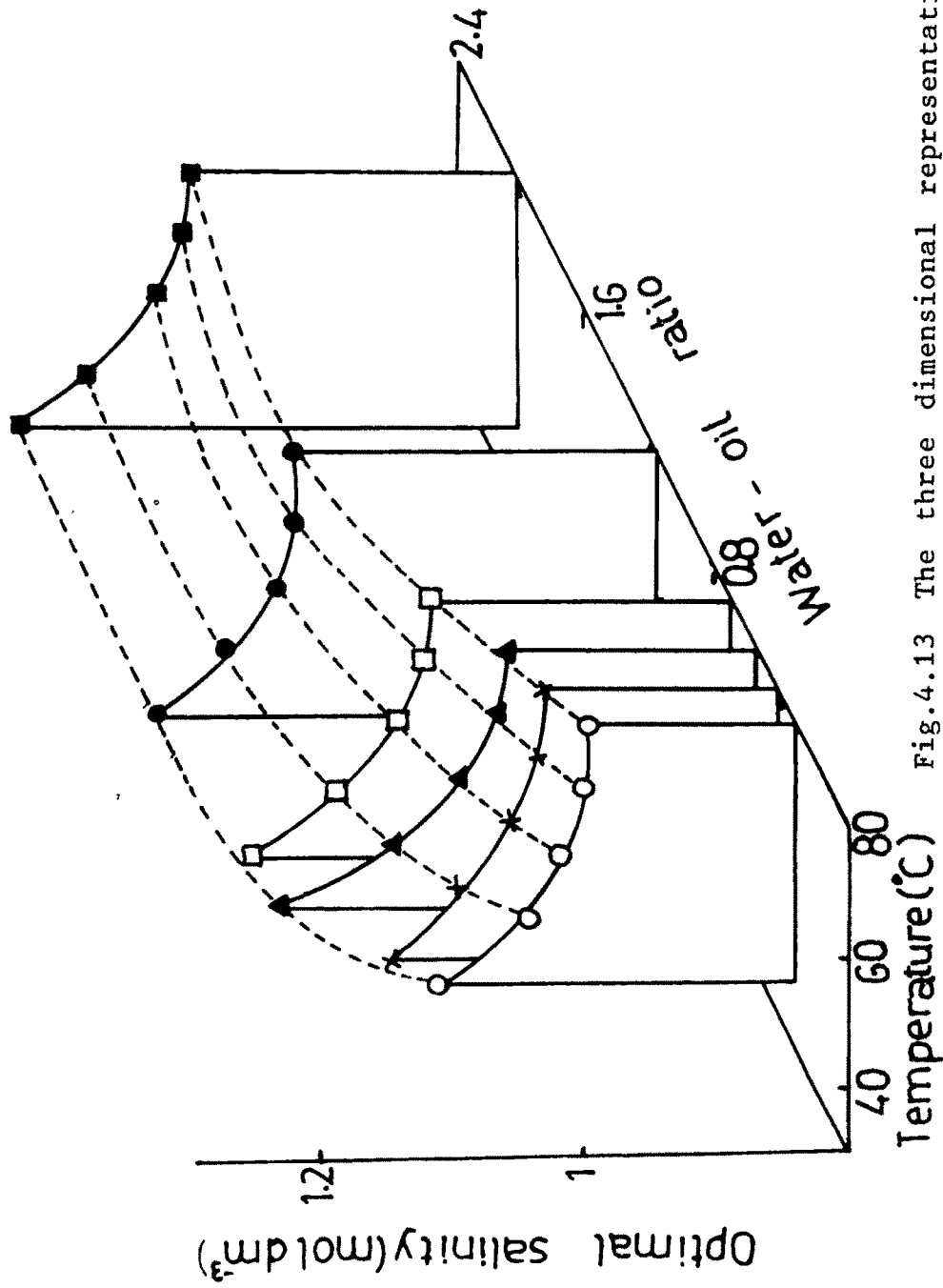


Fig.4.13 The three dimensional representation of the variation of optimal salinity with temperature and water-oil ratio.

the optimal salinity of these compositions with water-oil ratio at different temperatures. One can notice an increase in the optimal salinity with water-oil ratio at all temperatures and above a certain range of water -oil ratio, the salinity attains almost a constancy. Fig.4.13 is a comprehensive three dimensional representation of the optimal salinity with changing parameters i.e. temperature and water-oil ratio.

Fig.4.14 shows the interfacial tension (IFT), measured between the middle microemulsion layer (M.L) and equilibrated excess oil layer (U.L) or excess water layer (L.L) as a function of water -oil volume ratio in presence of 1.2 mol dm^{-3} salinity. Since this salinity is above the optimal salinity of the compositions, the microemulsion layer (M.L), though bicontinuous, is comparatively rich with oil. This creates fairly high interfacial tensions between M.L and aqueous L.L. and low interfacial tension values between M.L and organic U.L. initially at low water-oil ratio. As the optimal salinity increases on increasing the water-oil ratio, the salinity (1.2 mol dm^{-3}) becomes more closer to the optimal. This will cause the spontaneous expulsion of excess oil from the middle phase to attain a state of balance between its oil-water content and thereby concomitant decrease and increase in the tensions at the M.L/L.L. and M.L/U.L interfaces

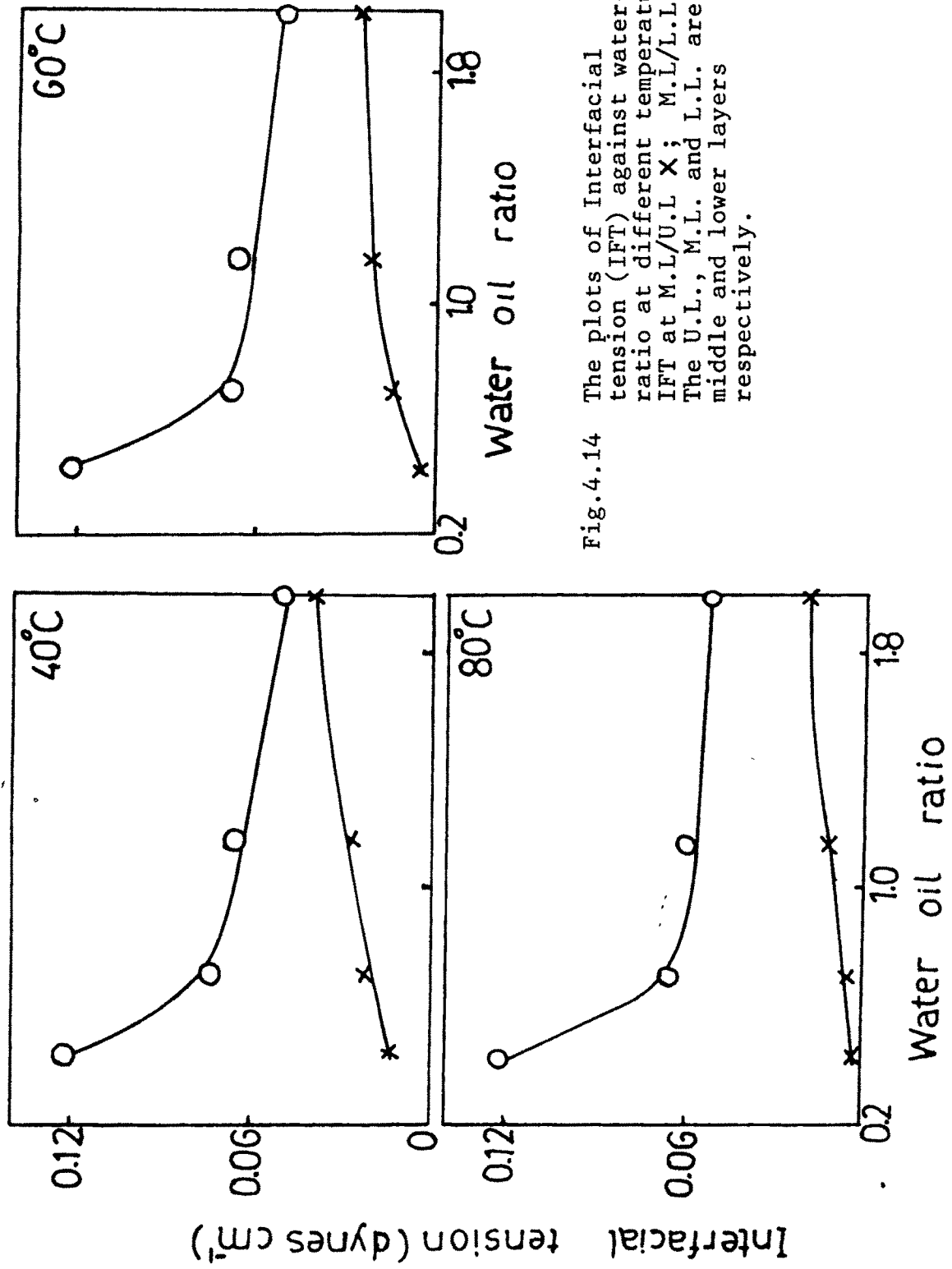


Fig.4.14 The plots of Interfacial tension (IFT) against water-oil ratio at different temperatures. IFT at M.L./U.L. X; M.L./L.L. O The U.L., M.L. and L.L. are upper middle and lower layers respectively.

respectively. This effect should be more prominent at higher temperatures, as the gap between the salinity and optimal salinity is more (Because the optimal salinity decreases with temperature). The diminished interfacial tension values between the M.L. and U.L. observed at higher temperatures are consistent to the above argument. But the effect of temperature increase may compensate the above mentioned effect on the M.L. - L.L interface and therefore does not produce large effect on the related IFT values.

(ii) Property study of 0.5 mol dm^{-3} NaCl system

In presence of 0.5 mol dm^{-3} NaCl, the one phase microemulsion (Winsor IV) forms as a single region across the pseudoternary phase diagram touching the oil corner on one side and water-surfactant base line on the other (Fig.4.2). Hence it was possible to study the properties systematically selecting various compositions along the entire region. In Fig.4.15 the specific conductance of microemulsion samples along the region is recorded against their water volume fraction. These profiles exhibit the percolation phenomenon at different constant temperatures. The existence of all the three microstructural regimes namely w/o, bicontinuous and o/w can be evidenced from the nature of the plots. The w/o and o/w microemulsions are

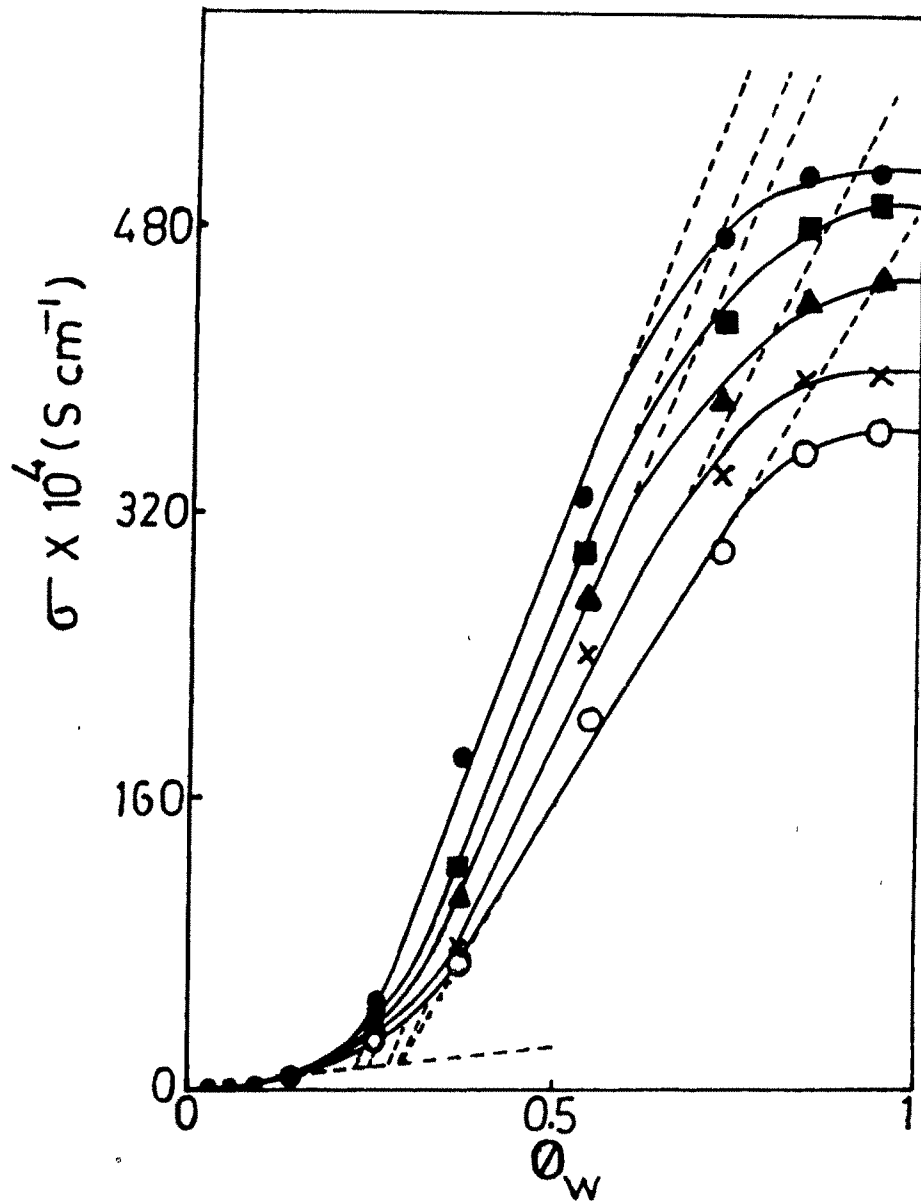


Fig. 4.15 The plots of specific conductance (σ) of microemulsion against water (0.5 mol dm^{-3} NaCl solution) volume fraction (ϕ_w) at various temperatures. 30°C ○; 40°C ×; 50°C ▲; 60°C ■; 70°C ●.

distinguished from their very low and high conductance respectively while the linear conductance variation in between, projects droplet fusion and the continuous water channel formation through which material propagation is possible. Comparison of this percolative pattern with pure water system (Chapter 3) shows that though the overall conductance values of the former are higher than the latter the order of increase in conductance during percolation phenomenon, with respect to oil continuous region, has diminished by the presence of NaCl. This was computed from the intersection of two sets of straight lines (dashed) at the lower region of the graphs (see Fig.4.15) and is compared in Table 4.1. From Table 4.1 it is observed that the ratio of the order decreases with increase in temperature. A plot of this ratio with temperature was found to be linear (Fig.4.16). This also indicates that at temperature $\sim 75^{\circ}\text{C}$, the ratio becomes unity indicating no effect of NaCl at this or at higher temperatures.

Kirk-Patrick [178] developed a satisfactory approach towards percolative conduction phenomenon exhibited by a conductor - nonconductor inhomogeneous media, which was latter applied to microemulsion systems by Lagourette et al.[179]. The variation of specific conductance σ with dispersed water volume fraction ϕ_w can be described by the

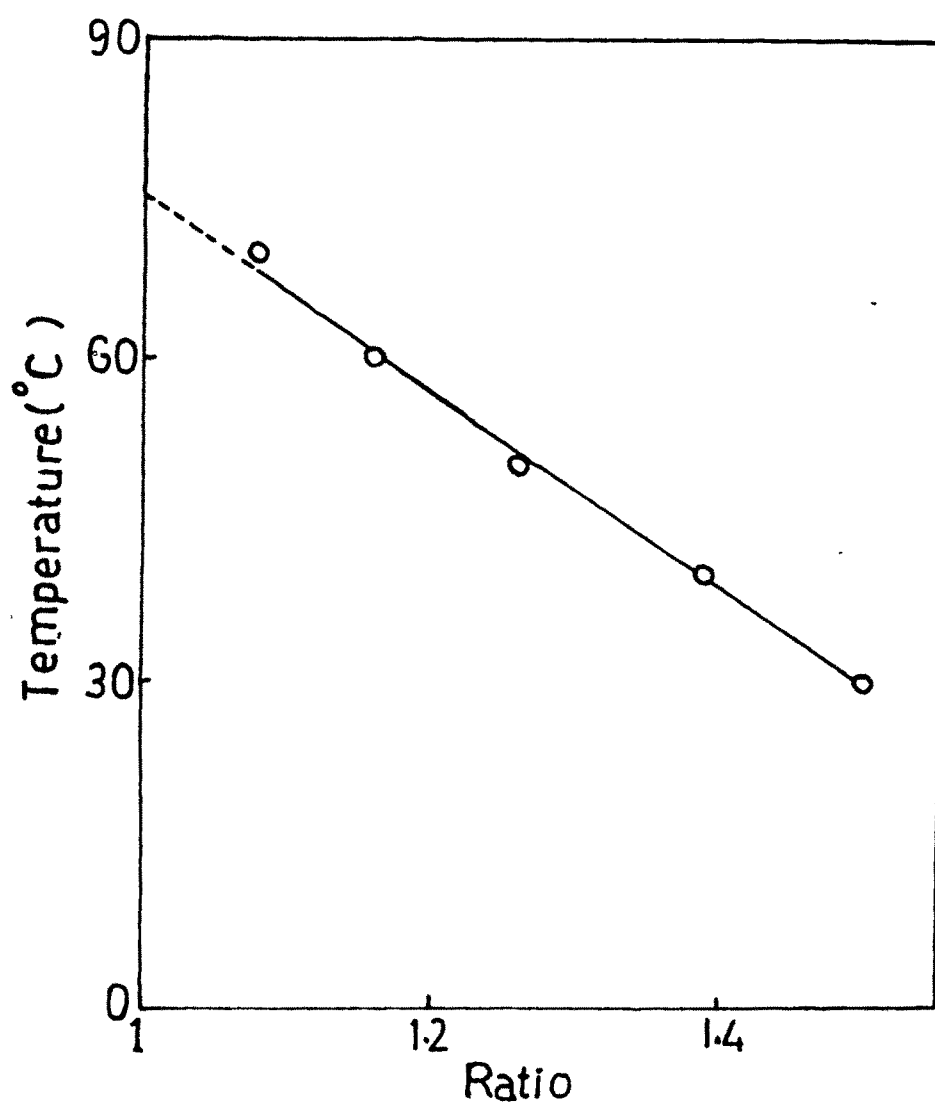


Fig. 4.16 The plot of the ratio of order of increase in conductance during percolation in water to that of 0.5 mol dm^{-3} NaCl solution against temperature (cf. Table 4.1)

TABLE 4.1

Approximate order of increase in specific conductance during percolation phenomenon for (a) water system (without NaCl) and (b) 0.5 mol dm⁻³ aqueous NaCl system

Temperature (°C)	Water System (a)	0.5 mol dm ⁻³ NaCl system (b)	Ratio (a/b)
30	39	26	1.50
40	43	31	1.39
50	48	38	1.26
60	52	45	1.16
70	56	52	1.08

scaling equation [180].

$$\sigma \propto (\phi_w - \phi_w^p)^t \quad (1)$$

where ϕ_w^p is the percolation threshold. The exponent 't' depends upon the value of ϕ_w . For low values of ϕ_w i.e. in the vicinity of percolation threshold, 't' assumes the value 8/5 but changes to unity at higher values of ϕ_w and the equation takes up the form (2) and (3) correspondingly.

$$\sigma \propto (\phi_w - \phi_w^p)^{8/5} \quad (2)$$

$$\sigma \propto (\phi_w - \phi_w^p) \quad (3)$$

The validity of equation (3) overlaps that of equation (2). In accordance with the equation (2), on plotting $\sigma^{5/8}$ against water fraction ϕ_w in the present system, we found that the middle portion of the plot can be termed a straight line (Fig.4.17) and the observed results seem to fit the equation (2). The intersection of this straightline with the ϕ_w axis provides ϕ_w^p , the percolation threshold [179]. The ϕ_w^p values were determined for the system at various temperatures and are compared with the corresponding values for pure water (Table 4.2). The shift in the percolation threshold values towards higher water fraction predicts an expansion in the w/o structural regime. This is consistent with the increased hydrophobicity of the surfactant in the presence of added

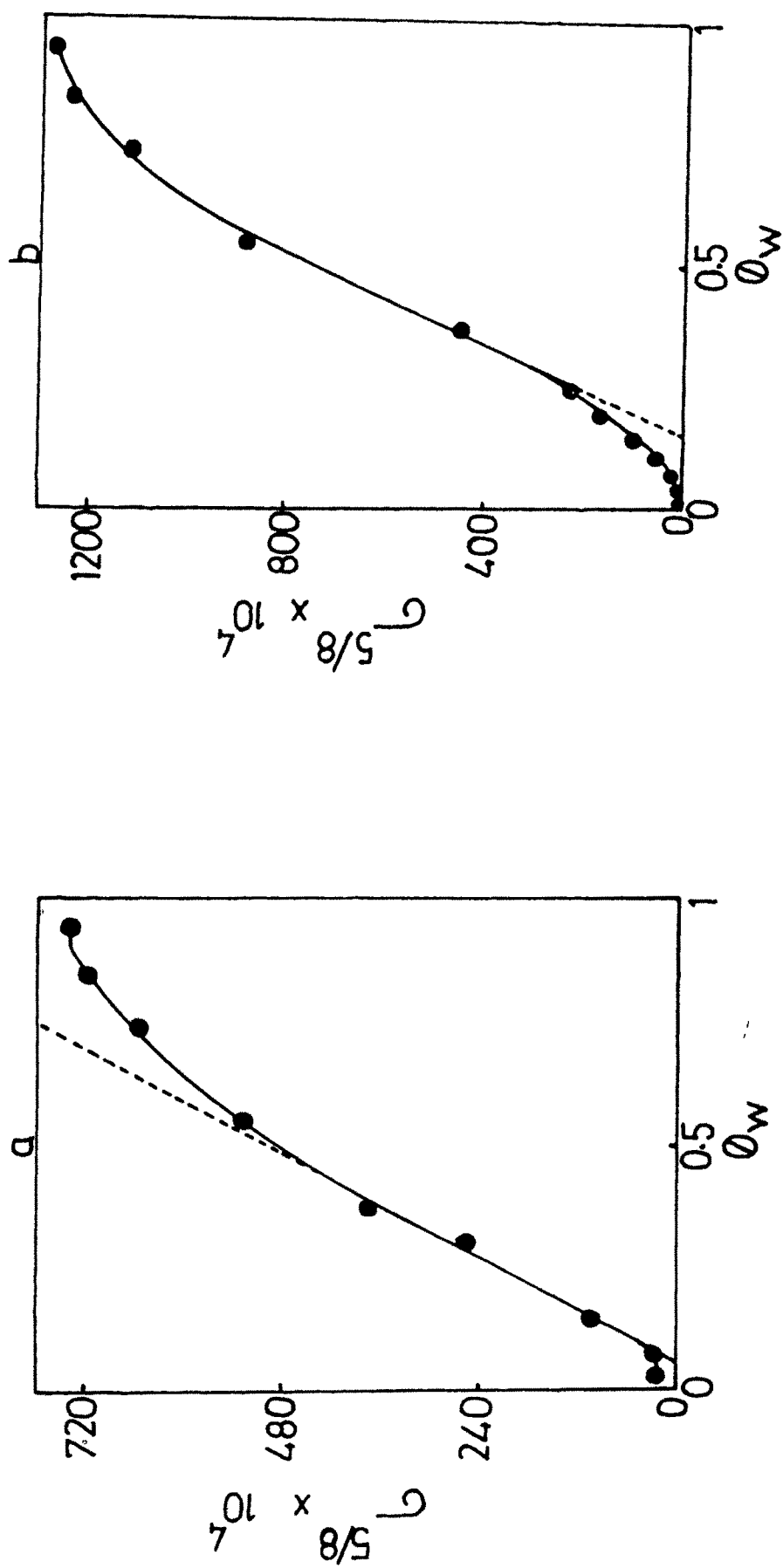


Fig.4.17 The plots of $\sigma^{5/8}$ against water volume fraction (ϕ_w) at 30°C for (a) pure water and (b) 0.5 mol dm⁻³ NaCl solution.

TABLE 4.2

Percolation threshold (ϕ_w^p) in terms of water volume fraction for (a) water system (without NaCl) and (b) 0.5 mol dm⁻³ NaCl system.

Temperature (°C)	ϕ_w^p		Ratio (a/b)
	pure water system (a)	0.5 mol dm ⁻³ NaCl system (b)	
30	0.05	0.15	0.33
40	0.05	0.14	0.36
50	0.06	0.16	0.38
60	0.06	0.15	0.40
70	0.06	0.14	0.43

NaCl: It is also observed that the ratio of ϕ_w^P in water to that in 0.5 mol dm^{-3} solution is somewhat a linear function of temperature and increases with increase in temperature (Fig.4.18).

It is the interaction between droplets which plays a major role in producing the percolation effect. Due to the attractive interaction between droplets, water channel formation occurs through which the ions move. The more channel means higher conductance and sudden increase indicates percolation process [152,181]. Depending on the interaction, the percolation threshold value ϕ_w^P can vary. This threshold value decreases when droplet interaction increases [182]. It has been observed earlier that a decrease in salt content can increase the droplet interaction which infact result in a decrease in the threshold [182]. On the other hand increasing addition of salt can minimize the interaction between the droplets and thereby create a threshold increase. This has been verified by Boned and Peyrelasse [181]. The lower the interaction the lesser the temporary droplet merging and hence formation of the water channels during clustering. The increased ϕ_w^P values obtained in the present study for 0.5 mol dm^{-3} NaCl tally well with the above argument. The rapid increase of conductance in presence of NaCl is of lesser order than in the case where NaCl is absent. This

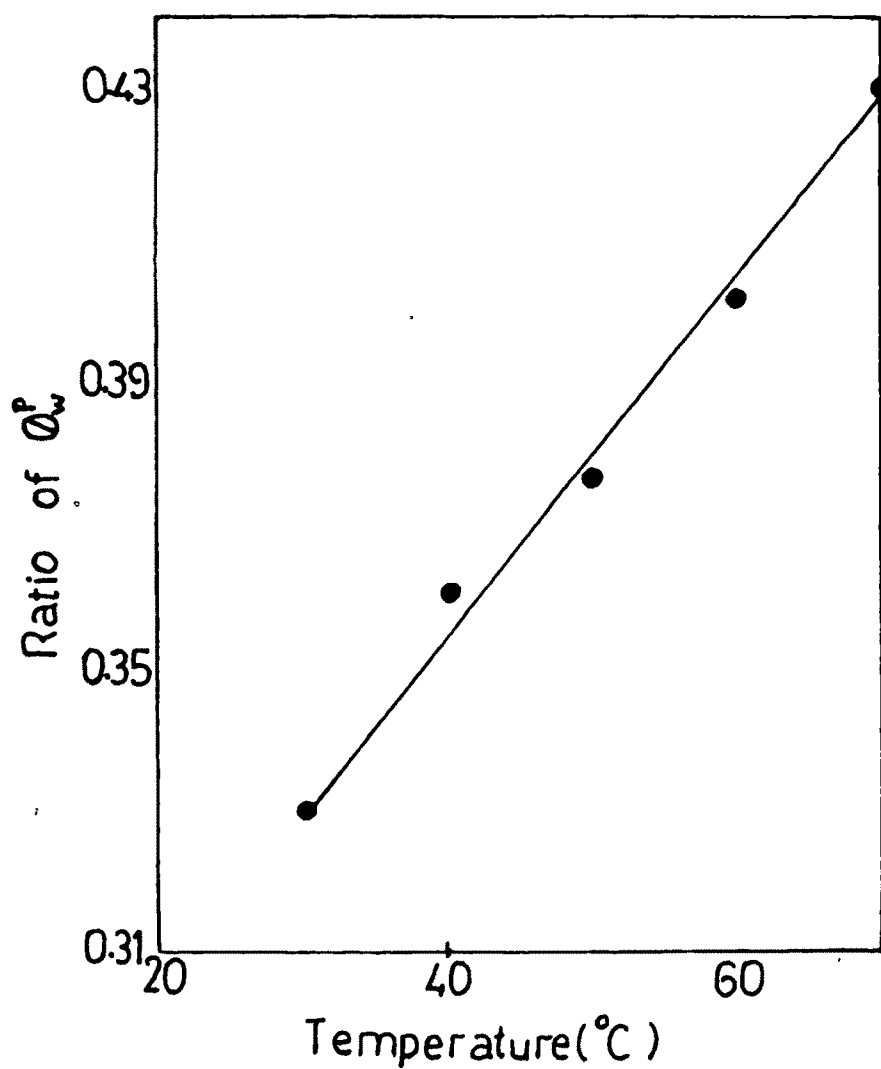


Fig. 4.18 The plot of the ratio of percolation threshold (ϕ_w^p) in water to that of 0.5 mol dm^{-3} NaCl solution as the function of temperature (cf. Table 4.2).

may be due to the decreased interaction between the droplets.

In Fig.4.19 the variation of conductance with increasing temperature for four different w/o microemulsion samples with water to oil ratio 0.05, 0.08, 0.12 and 0.16 are illustrated. Like pure water system these 0.5 mol dm^{-3} NaCl containing system also exhibit a declining trend in conductance for these w/o samples. But it is worthwhile to note that the decrease is more orderly and with increasing water-oil ratio the trend gradually reverses with the samples lying above the water percolation threshold showing an ascending trend with temperature. This decrease in electrical conductivity of w/o microemulsions is also attributed to the short time span spend by each droplet near the other at higher temperatures and decreased probability of ion hopping as described in chapter 3. But as the water concentration increases the population of water globules becomes large enough to emerge as continuous channels with temperature increase and hence the increase in conductance. From this we believe that the low electrical conductivity exhibited by w/o microemulsions is mainly due to a dynamic hopping mechanism [183] of ions through the globules whereas above the percolation threshold a sticky collision leading to the droplet fusion holds the responsibility.

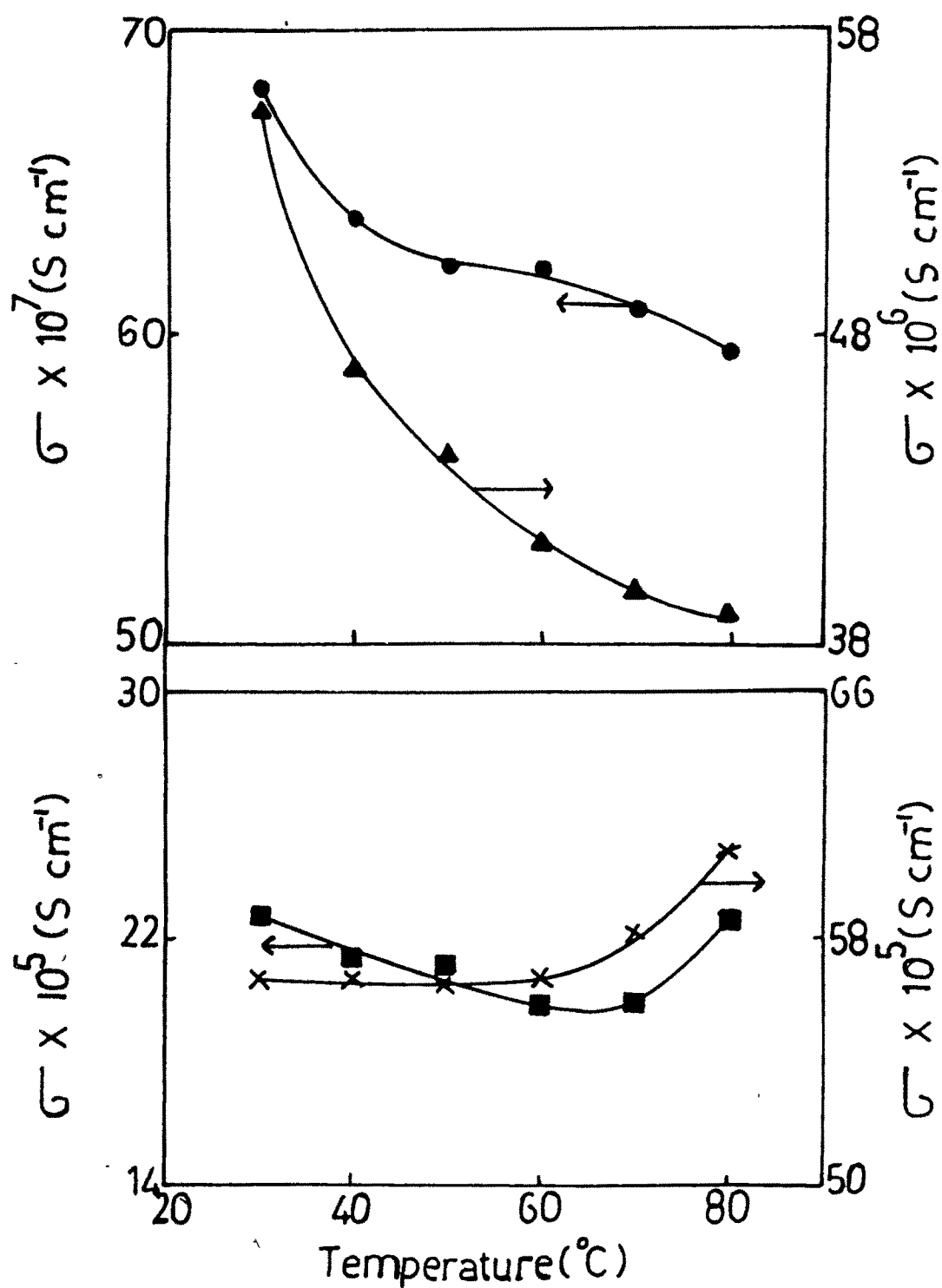


Fig. 4.19 The plots of specific conductance (σ) against temperature for four w/o microemulsion samples of different water oil ratios : 0.05 ● ; 0.08 ▲ ; 0.12 ■ ; 0.16 × .

The viscosity measurement carried out along the 42.5 percentage surfactant composition line of the phase diagram (Fig.4.20) also confirms the existence of bicontinuous and o/w structures in this system in presence of 0.5 mol dm^{-3} NaCl. The steady increment in the viscosity with water fraction signifies the bicontinuous structure and the obtained peaks mark the transition to o/w structure. The measured viscosity values of various compositions in this system are shown with the corresponding values in the pure water system for comparison in Table 4.3. A suppression, though not very large, in the viscosity values can be observed in presence of NaCl. The specific role of salts in reducing the viscosity is apparent since it can reduce the attractive interaction of fluid interfaces [184] and also screen the interactions between the dispersed phase microdomains. Further the added salts can break up the possible intermolecular hydrogen bondings between the alcohol and water or water and water as described by Keiser et al.[52].

The adiabatic compressibility (β) measured along the 42.5 percent surfactant composition line of the phase diagram is provided in Fig.4.21 as the function of volume fraction of aqueous NaCl solution. The obtained plots are typical of pure water system and do not provide much

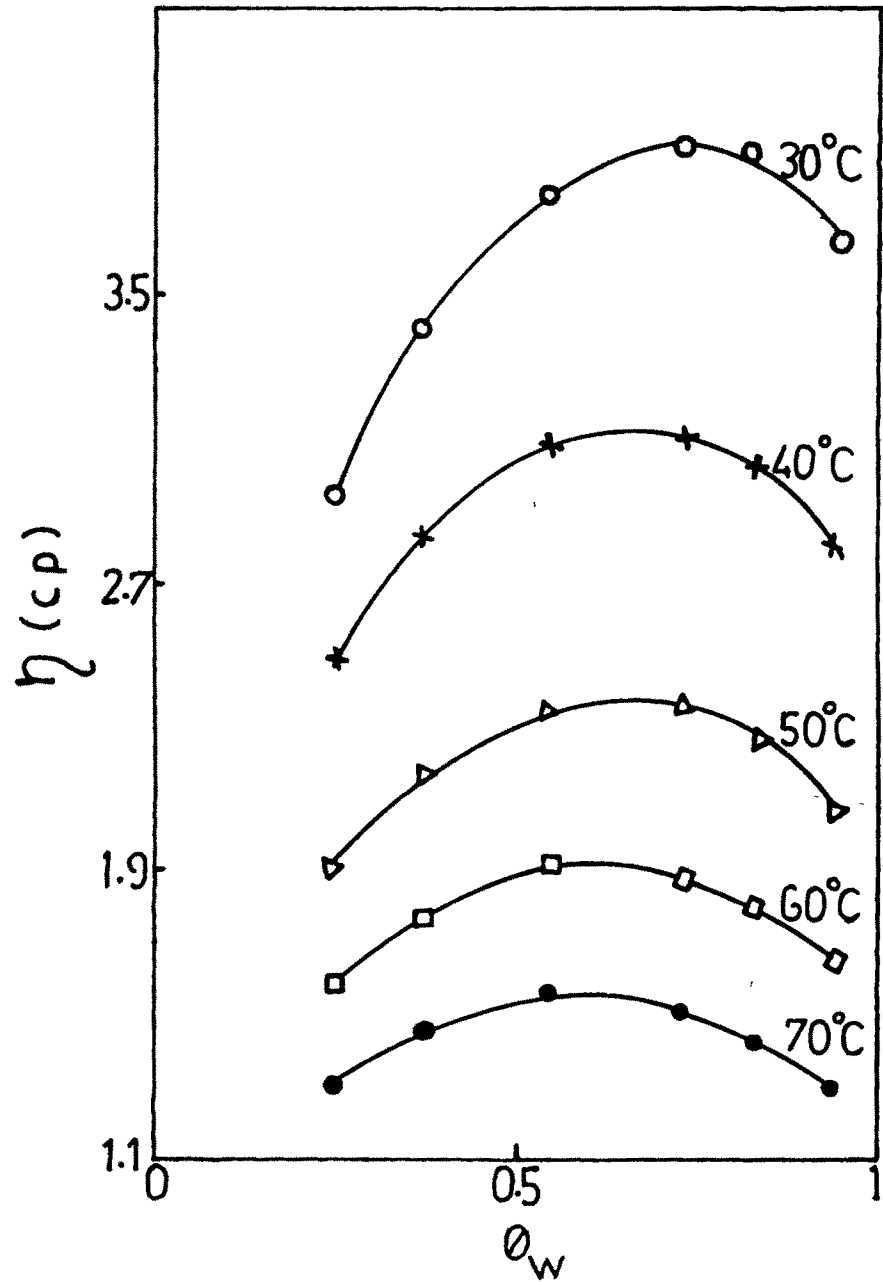


Fig.4.20 The variation of viscosity (η) as the function of 0.5 M aqueous NaCl volume fraction (ϕ_w) at constant surfactant 42.5 weight percent.

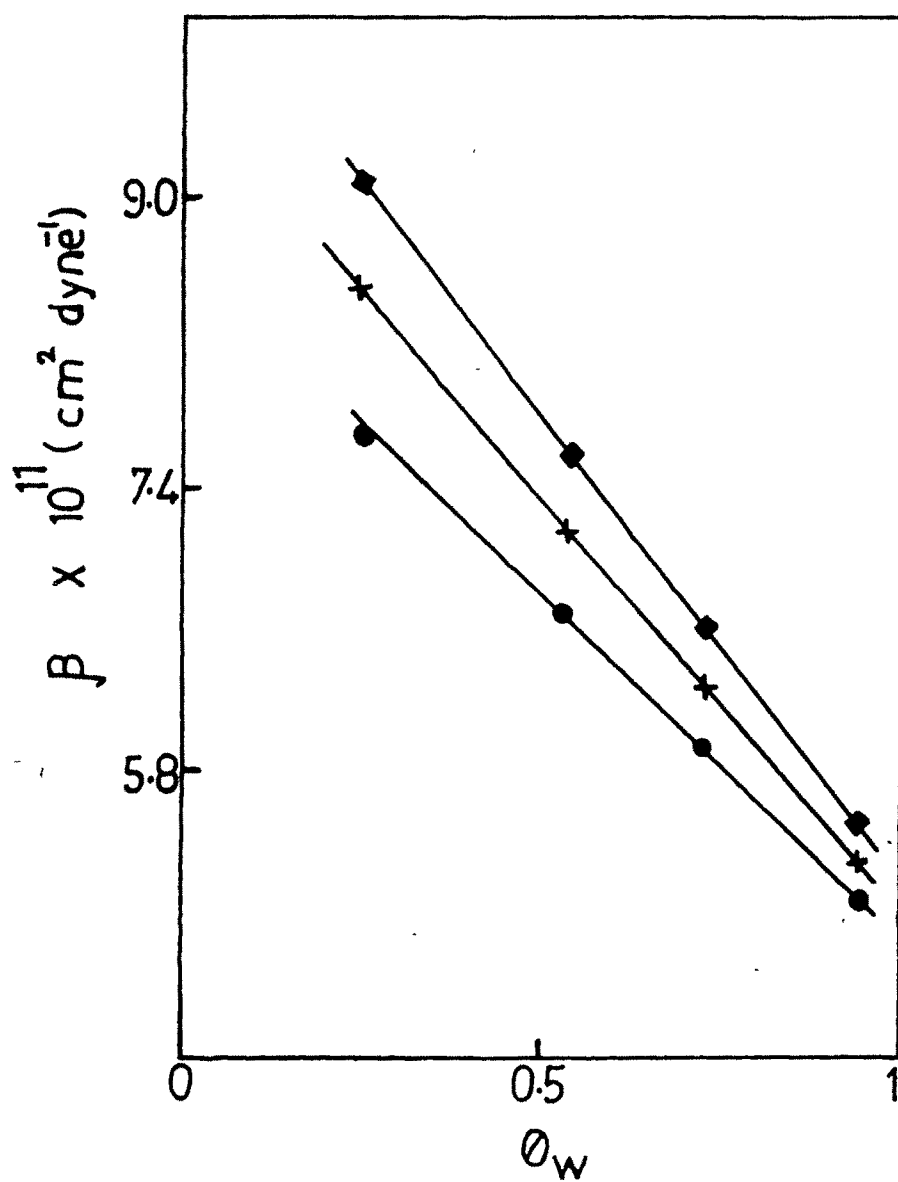


Fig.4.21 The plots of adiabatic compressibility (β) vs water (0.5 M NaCl) volume fraction (ϕ_w) at constant surfactant percentage 42.5, and different temperatures 30°C ●; 40°C X; 50°C ■.

TABLE 4.3

Viscosity of various compositions in presence and absence of NaCl.

Composition in weight percentage S+CS/O/W	Viscosity of pure water system (cP)					Viscosity of 0.5 mol dm ⁻³ NaCl system (cP)				
	30°C	40°C	50°C	60°C	70°C	30°C	40°C	50°C	60°C	70°C
42.5/2.5/55	3.70	2.91	2.14	1.68	1.34	3.62	2.81	2.07	1.65	1.29
42.5/7.5/50	3.99	3.14	2.30	1.80	1.42	3.91	3.03	2.25	1.80	1.42
42.5/12.5/45	4.03	3.22	2.38	1.87	1.48	3.88	3.11	2.36	1.85	1.48
42.5/22.5/35	3.89	3.17	2.39	1.92	1.56	3.78	3.11	2.37	1.92	1.56
42.5/32.5/25	3.49	2.89	2.21	1.79	1.51	3.41	2.84	2.19	1.78	1.46
42.5/40/17.5	3.22	2.58	1.99	1.62	1.36	2.96	2.49	1.91	1.57	1.30

insight into the microstructural diversions. Rather it seems to be a bulk property depending on the oil or water content. The decreasing β values with increasing water content is because of the lesser compressibility of water compared to oil. In addition, in presence of NaCl, as the water concentration decreases, the salt containing water domains become more spread in the hydrocarbon environment and therefore interparticle interaction becomes less. This will impart overall softness to the system [83]. The comparison of values obtained in presence of NaCl to pure water values reveals that the microemulsion turns slightly rigid (decrease in β) in presence of the salt (Table 4.4). When the repulsive interaction between the surfactant head groups is screened by the presence of salt, the hydrocarbon tail region of the interfacial film is viable to be penetrated by increased number of oil molecules. This will result in a more rigid interfacial layer and thereby overall structure [59]. The compressibility versus temperature plot (Fig.4.22) suggests a more loosened structure for the samples at elevated temperature. The closed packing of the amphiphile molecules in the interfacial film gets disturbed by the increased thermal motion at higher temperature [64]. This will swell up the interfacial layer and impart less rigidity.

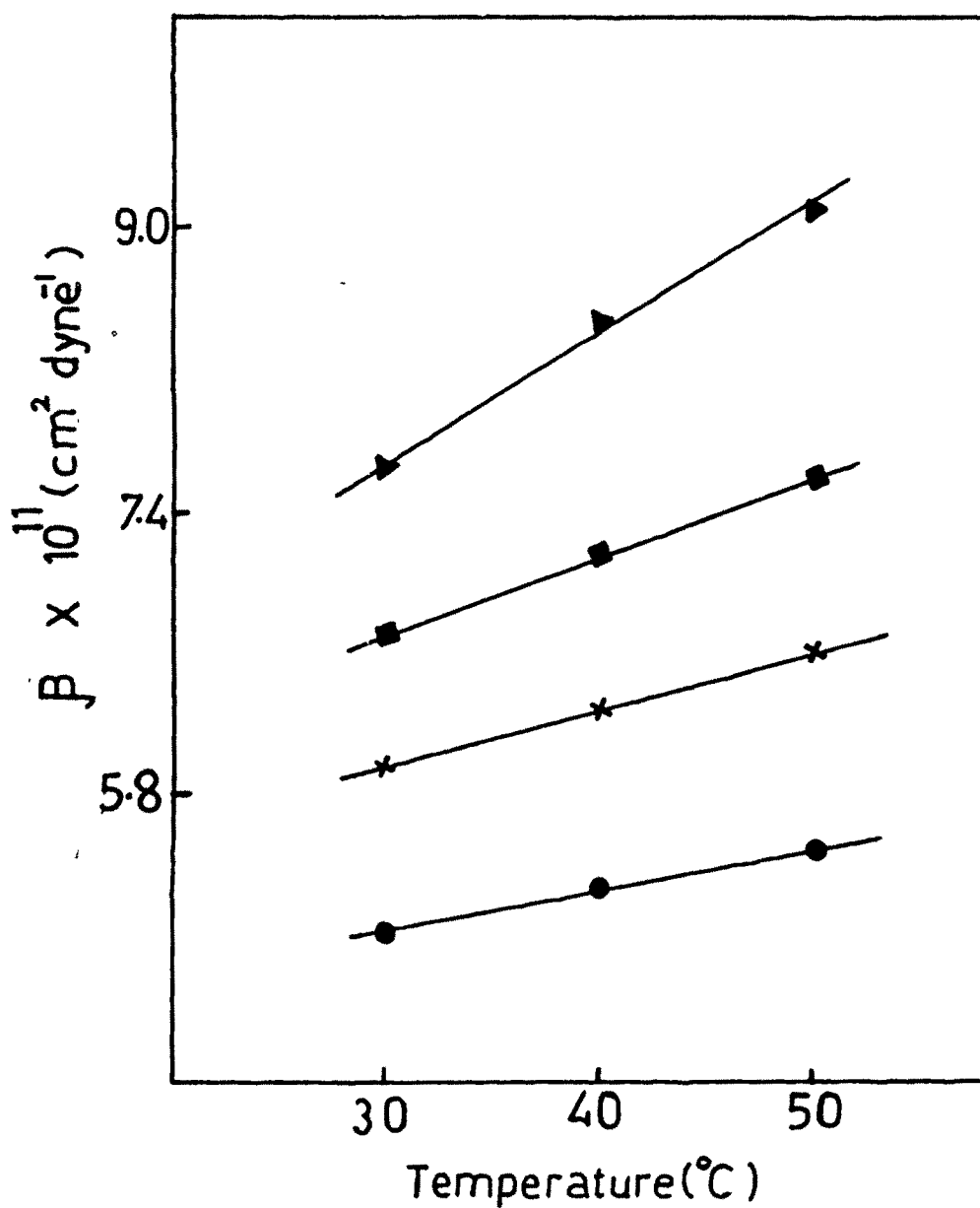


Fig.4.22 The variation of adiabatic compressibility (β) against temperature for microemulsions with 0.5 M aqueous NaCl solution and varying water-oil ratios 22 ●; 3.6 ×; 1.56 ■; 0.44 ▲.

TABLE 4.4

Adiabatic compressibility of microemulsion compositions in presence and absence of NaCl.

Composition in weight percentage S+CS/O/W	Adiabatic compressibility $\beta \times 10^{11} \text{ cm}^2/\text{dynes}$					
	Pure water system			0.5 mol dm ⁻³ NaCl system		
	30°C	40°C	50°C	30°C	40°C	50°C
42.5/40/17.5	7.80	8.50	9.12	7.66	8.49	9.08
42.5/22.5/35	6.76	7.18	7.63	6.72	7.16	7.58
42.5/12.5/45	6.05	6.33	6.73	5.97	6.27	6.60
42.5/2.5/55	5.16	5.36	5.61	5.05	5.27	5.50

(iii) Property study of 1 mol dm^{-3} NaCl system

In presence of 1 mol dm^{-3} NaCl, the monophasic region lies adjacent to the surfactant-water base line of the ternary phase diagram (Fig.4.3). Conductance, viscosity and compressibility studied in this region along a line, where the weight percentage of oil was kept constant (2.5) are shown against their water mass fraction in Figures 4.23, 4.24 and 4.25 respectively. Unlike in the case of 0.5 mol dm^{-3} NaCl system, no major structural diversity or phenomena is evidenced from these profiles. The conductance, though slightly curved at low temperature, increases regularly in a linear fashion at higher temperatures (Fig.4.23). Starting from a high surfactant containing region, on adding water the system transforms itself from a probable surfactant continuous to a more water continuous state. During this dilution process, an increase in both the number of water channels and the medium dielectric constant may be responsible for the smooth increase in the conductivity. The obtained viscosity versus water mass fraction profiles (Fig.4.24) are complementary to the observed conductance variation according to the Walden rule in electrolyte solutions. But the Walden product which is constant for an electrolyte solution does not remain so in this case. However it is different that the earlier observations [68,83] where

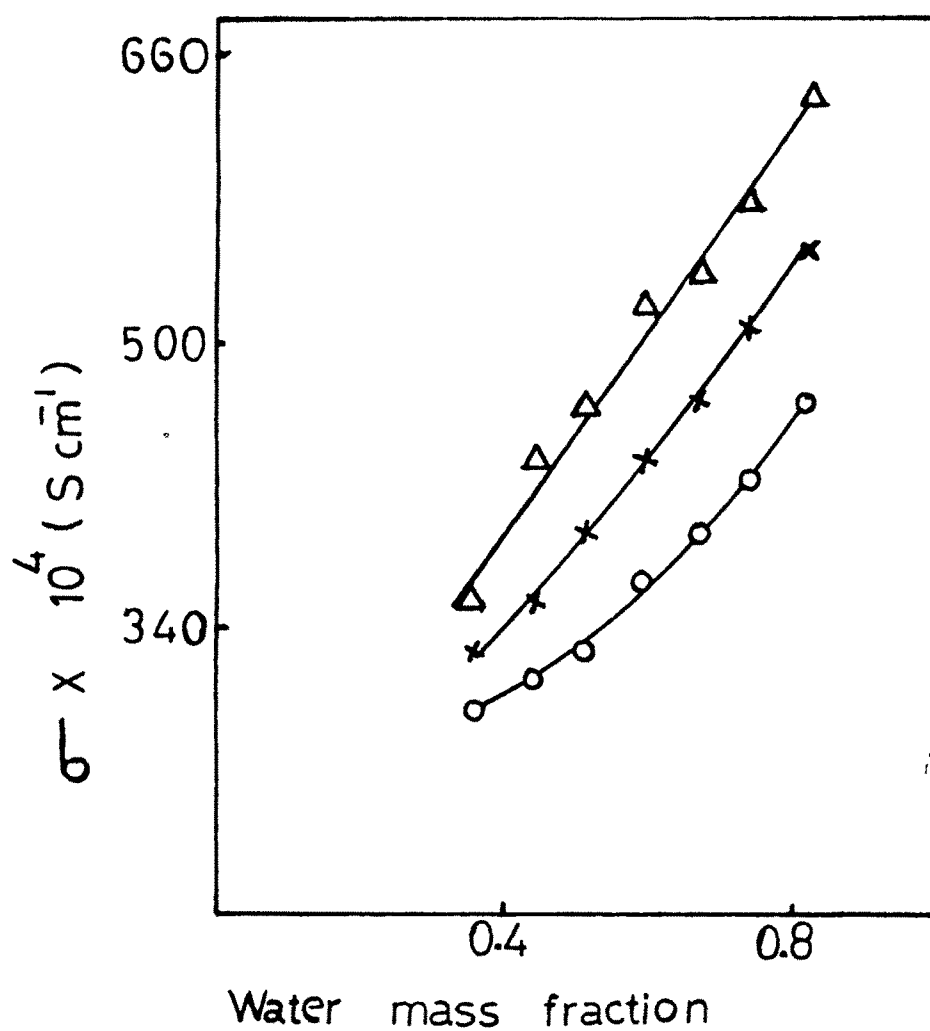


Fig.4.23 The variation of specific conductance (σ) against water ($1 \text{ mol dm}^{-3} \text{ NaCl}$) mass fraction along a line, of constant oil percentage 2.5, in the phase diagram at different temperatures. 30°C O ; 50°C X ; 70°C Δ .

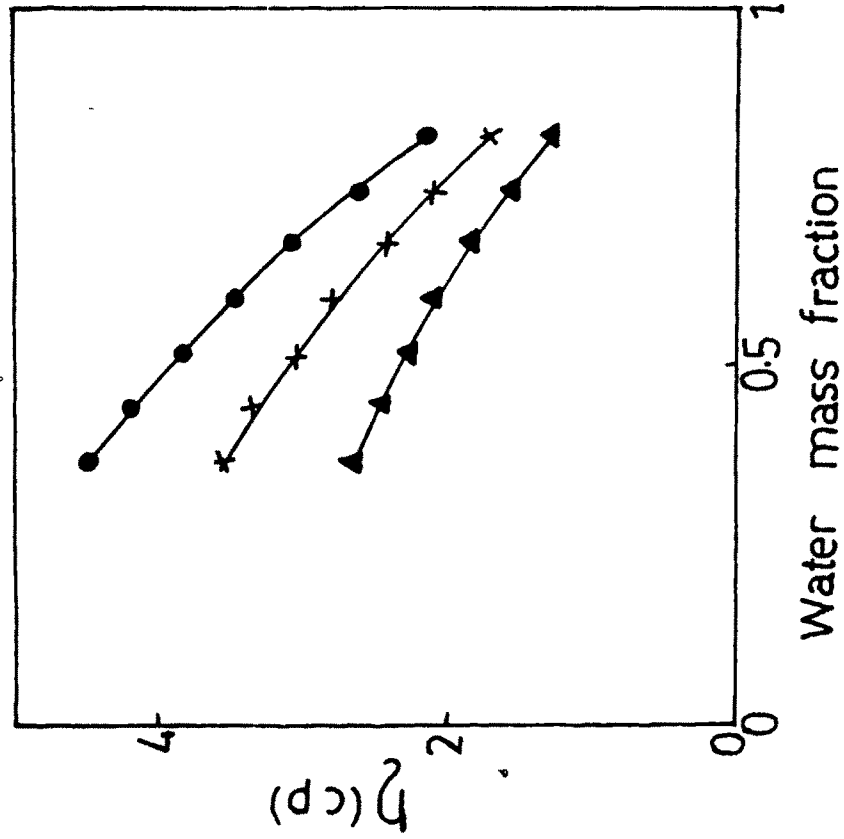


Fig.4.24

The plots of microemulsion viscosity (η) vs water (1 M NaCl) mass fraction at constant oil weight percentage 2.5, at different temperatures 30°C ●; 40°C X; 50°C ▲.

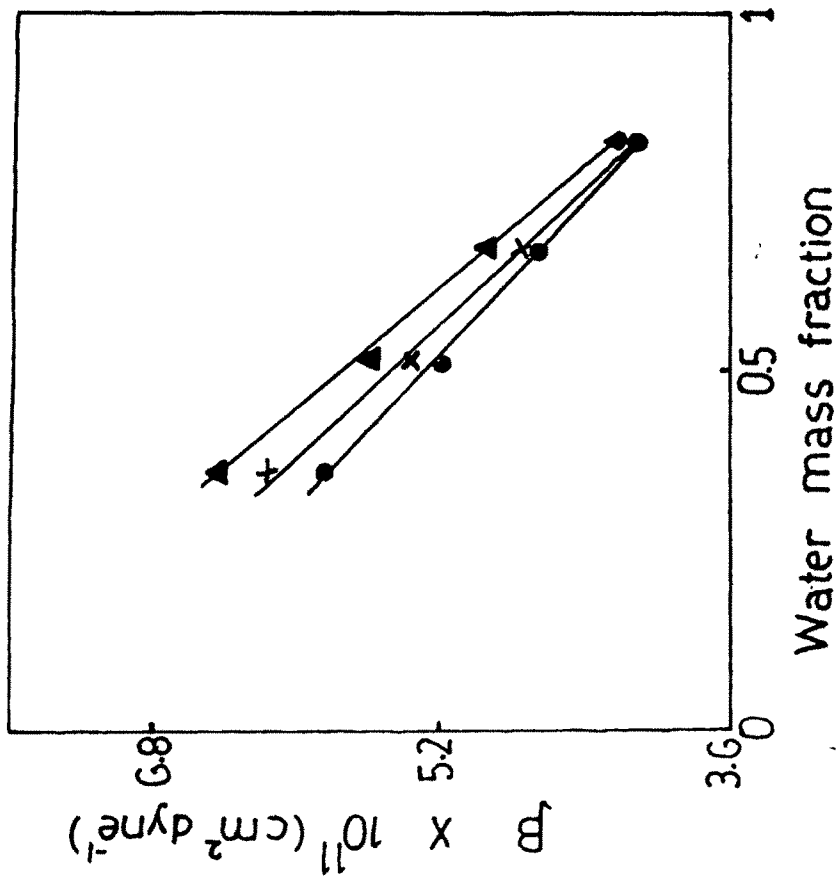


Fig.4.25

The variation of adiabatic compressibility against water (1 M NaCl) mass fraction at constant oil percentage 2.5, at temperatures 30°C ●; 40°C X; 50°C ▲.

simultaneous increase in both the transport properties were observed. The compressibility decrease with increasing water content (Fig.4.25) is in agreement with the earlier observation (Chapter - 3) of more ordered and rigid structure when water is more.